How far is far from critical point in polymer blends? Lattice cluster theory computations for structured monomer, compressible systems

ARTICLE *in* THE JOURNAL OF CHEMICAL PHYSICS · SEPTEMBER 1993

Impact Factor: 2.95 · DOI: 10.1063/1.466028

4 AUTHORS, INCLUDING:

Karl F. Freed
University of Chicago
657 PUBLICATIONS **16,394** CITATIONS
SEE PROFILE

J. F. Douglas
National Institute of Standards and Tech…
428 PUBLICATIONS **14,795** CITATIONS
SEE PROFILE

How far is far from critical point in polymer blends? Lattice cluster theory computations for structured monomer, compressible systems

Jacek Dudowicz, Masha Lifschitz, Karl F. Freed, and Jack F. Douglas

Citation: The Journal of Chemical Physics **99**, 4804 (1993); doi: 10.1063/1.466028
View online: http://dx.doi.org/10.1063/1.466028
View Table of Contents: http://scitation.aip.org/content/aip/journal/jcp/99/6?ver=pdfcov
Published by the AIP Publishing

How far is far from critical point in polymer blends? Lattice cluster theory computations for structured monomer, compressible systems

Jacek Dudowicz, Masha Lifschitz, and Karl F. Freed
The James Franck Institute and the Department of Chemistry, University of Chicago, Chicago, Illinois 60637

Jack F. Douglas
Material Science and Engineering Laboratory, National Institute of Standards and Technology, Polymer Division, Gaithersburg, Maryland 20899

(Received 14 May 1993; accepted 10 June 1993)

Although the lattice cluster theory (LCT) incorporates many features which are essential in describing real polymer blends, such as compressibility, monomer structures, local correlations, chain connectivity, and polymer–polymer interactions, it still remains a mean field theory and is therefore not applicable in the vicinity of the critical point where critical fluctuations become large. The LCT, however, permits formulating the Ginzburg criterion, which roughly specifies the temperature range in which mean field applies. The present treatment abandons the conventional assumptions of incompressibility and of composition and the molecular weight independent effective interaction parameter χ_{eff} upon which all prior analyses of the Ginzburg criterion are based. Blend compressibility, monomer structure, and local correlations are found to exert profound influences on the blend phase diagram and other critical properties and, thus, exhibit a significant impact on the estimate of the size of the nonclassical region. The LCT is also used to test various methods which employ available experimental data in computations of the Ginzburg number Gi. The reduced temperature $\tau=|T-T_c|/T$ defining the range of the validity of mean field theory ($\tau>\tau_{\text{MF}}$) and the onset of the Ising-type scaling regime ($\tau>\tau_{\text{crit}}$) are quite different, and renormalization group estimates of τ_{MF} and τ_{crit} are presented as a function of Gi to more precisely specify these scaling regimes.

I. INTRODUCTION

Despite the limited portion of the phase diagram occupied by the critical region, the equilibrium and dynamic critical phenomena occurring in this regime have attracted considerable attention. The critical regime is especially interesting for theoretical study because large scale fluctuations can be described by a universal long wavelength theory. The primary focus of experimental and theoretical studies has been on critical exponents and amplitude ratios, characterizing large scale system properties in the scaling regime near the critical point. However, these properties are just the tip of the iceburg for the full range of critical behavior. In addition to the scaling region, there is a crossover regime between the asymptotic critical regime and the mean field region in which fluctuations are weak and the details of the molecular interaction become important. An understanding of the factors governing the size of the critical domain and this crossover is essential in developing a complete thermodynamic description of fluids and in interpreting experiments on critical dynamics and the dynamics of phase separation. The development of a global thermodynamic description[1] for equilibrium and dynamic properties of fluids also has many practical applications.[2] There are also basic questions regarding the matching of mean field and critical theories,[1] the description of how and why *mean* field theory breaks down, and the explanations of factors delineating the onset of critical behavior. Recent efforts have thus been devoted to extending the scope of critical phenomena to include the transition from Ising-type to mean field critical behavior.

High molecular weight polymers are excellent systems for studying the size of the critical region because the variation of the polymerization index allows for control of the size of the critical domain, a control which is impossible with small molecule fluids. Theories for the size of the critical region in polymer systems have been developed using the incompressible random phase approximation (RPA) and incompressible Flory–Huggins (FH) theory with a composition independent interaction parameter χ_{eff}. These theories, originally due to de Gennes[3] and Binder,[4] generalize to polymers the famous Ginzburg criterion[5] for the size of the critical region, thereby delineating the domain in which mean field descriptions are valid. Based on these theories, it is widely believed that mean field theory becomes exact for polymer blends in the limit of infinite molecular weights and that there is a growing Ising-like critical domain as the molecular weights decrease towards the small molecule limit. Experiments by Herkt-Maetzky and Schelten[6] demonstrate the crossover to a nonclassical regime in polymer blends and thereby provide the first verification of the theoretical predictions.

Bates *et al.*[7] have extended the original theory to formulate a FH–Ginzburg criterion for binary blends of polymers with different polymerization indices and Kuhn lengths for the two blend components. They report "quan-

 0021-9606/93/99(6)/4804/17/$6.00

titative agreement" of this criterion with their experiments[7] on polyisoprene/poly(ethylene–propylene) blends. Specifically, if T_c is the critical temperature and $\tau = |T - T_c|/T$ measures the deviation from the critical point, Bates *et al.* note that the temperature at which the neutron (or light) scattering data begin exhibiting deviations from conventional mean field behavior occurs for τ closely coinciding with the predictions based on computations of the Ginzburg number[5] Gi from incompressible FH-RPA theory, predictions indicating that there is a universal criterion for the size of the critical domain.

Several subsequent experimental studies,[8–12] however, fail to find the universal behavior predicted by the FH–Ginzburg criterion of Bates *et al.*[7] An alternative modification of the FH–Ginzburg criterion by Hair *et al.*[11] seeks to redress the problem by incorporating directly observable quantities into the definition of the Ginzburg number in an attempt to correct partially for inadequacies of the FH and RPA theories. Hair *et al.*'s[11] expression for Gi contains, however, a fourth derivative of the free energy, which cannot be determined directly from experimental neutron or light scattering data. Hair *et al.*[11] are thus forced to evaluate this derivative employing incompressible FH theory with a composition and molecular weight independent χ_{eff}. Fisher[13] has also emphasized the importance of a better understanding of the Ginzburg criterion for the size of the critical region in micellar liquids. Consequently, it is clear that further theoretical and experimental studies of the cross-over regime in polymer systems are required to enable a more accurate estimation for the size of the critical domain using readily accessible experimental information.

It is well known that incompressible FH theory with a composition independent χ_{eff} is an overly simplistic representation of real polymer blends. Hence, a first consideration of deficiencies in the FH–Ginzburg criterion should begin with lifting the incompressibility assumption. Indeed, some systems of interest have lower critical solution temperatures that can only be explained using theories for a compressible system. Comparisons of the lattice cluster theory (LCT) with experiment show[14] that in addition to lifting the approximation of incompressibility, a description of the thermodynamic properties of real polymer blends requires considering the influence of local correlations in the system and of monomer molecular structures, features which are absent in simple FH theory. A forthcoming paper[15] develops theoretical modifications necessary to determine the Ginzburg criterion for a compressible system using compressible Flory–Huggins theory (Sanchez–Lacomb theory[16]) and the compressible RPA of Tang and Freed.[17] The present paper extends this study by using LCT computations of the blend free energy, a more realistic description of a real polymer blend.

Our interest in developing the LCT–Ginzburg criterion for polymer blends is actually manifold. First of all, it is of interest to determine the influence of "equation of state effects," local correlations, and monomer structures (hence also a composition dependent χ_{eff}) on the Ginzburg number Gi and therefore on a quantitative measure for the size of the critical region. Second, it is important to test the new criterion against real blend data to determine the extent to which the more general theory provides useful estimates of the width of the nonclassical region for polymer blends. Third, the LCT may be used in conjunction with experimental data that are obtained far from the critical regime as a vehicle for extrapolating–interpolating the data to the critical point, where free energy derivatives are required in order to compute the Ginzburg number Gi. This procedure enables us to test various methods for handling available experimental data in computations of Gi. Fourth, the analysis uses LCT whose validity limits are established. Finally, we take this opportunity to provide additional examples of the fact that the temperature range in which mean field theory breaks down is quite distinct from the temperature at which full critical behavior is developed. Criteria delimiting these regimes are developed in terms of Gi using the results of renormalization group calculations (which will be presented elsewhere[18]) in conjunction with the LCT for computing bare quantities.

Section II briefly reviews some background on predictions of the LCT theory for binary polymer blends and the conditions, developed[15] in paper II for compressible blends, defining their phase stability and the critical point at constant pressure. Section III presents the Ginzburg criterion appropriate to compressible blends with structured monomers and introduces the renormalization group theory criteria delimiting the magnitude of the reduced temperatures τ_{MF} and τ_{crit} at which mean field theory is no longer applicable and at which critical behavior is exhibited, respectively. Section IV describes LCT computations of Ginzburg numbers for polystyrene/polyvinylmethylether (PS/PVME) and polystyrene/polymethylmethacrylate (PS/PMMA) blends. These blends are selected because they exhibit qualitatively different phase diagrams (with lower and upper critical solution temperatures, respectively) and because the microscopic energetic parameters $\{\epsilon_{\alpha\beta}\}$ necessary to determine the LCT free energy are known for these two systems from our previous LCT fits[14,19] to various experimental data.[20–22] Our detailed consideration of these blends leads to a number of interesting results. The phase diagrams for a series of PS/PVME blends with a fixed molecular weight ratio is shown to have an increasingly asymmetric form. Remarkably, the critical temperature for this blend varies with the polymerization index N_1 as $N_1^{-1/2}$, except for the very low molecular weight region. The phase diagrams of these blends thus display some resemblance to those for solutions of polymers in small molecule solvents,[23] where the asymmetry has an obvious geometrical origin in terms of the dissimilarity in dimensions of the solvent and polymer molecules. A separate examination is made of the dependence of the correlation length amplitude on molecular weights because of the importance of this parameter in determining the width of nonclassical region. The lattice cluster theory calculations for the molecular weight dependence of the size of the critical regime exhibit strong departures from classical theories, and analyses are made of various methods for utilizing experimental information to estimate this size.

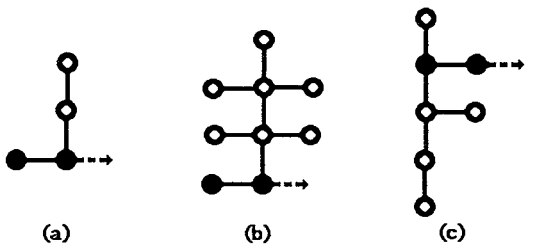

FIG. 1. A model of monomer structures for (a) vinylmethylether; (b) styrene; and (c) methylmethacrylate. Circles denote portions of monomers on single lattice sites and lines depict flexible bonds. Solid circles in monomer structures designate monomer portions lying on the backbone chain, and arrows indicate the directions of linkages between consecutive monomers in the polymer chains.

II. LATTICE CLUSTER THEORY OF A BINARY BLEND AT CONSTANT PRESSURE

A. Model of binary blend

The generalized lattice model of a binary blend depicts two polymer species $\alpha=1$ and 2 with polymerization indices N_α as n_α chains placed on a regular array with N_l total lattice sites and coordination number z. Individual monomers of both polymer species are connected by $N_\alpha-1$ flexible backbone bonds and each monomer occupies s_α neighboring lattice sites. The monomers are given prescribed architectures to reflect their relative sizes, shapes, and internal chemical structures. Consequently, the site occupancy index $M_\alpha=N_\alpha s_\alpha$ emerges as an additional variable which, in conjuction with the monomer structures, specifies more accurately the polymer species α than just the polymerization index N_α of the traditional lattice model. The site occupancy index M_α is the number of lattice sites covered by a single chain of species α, and the total number of occupied lattice sites then equals $N_{\rm occ}=n_1M_1+n_2M_2$. The occupation number $N_{\rm occ}$ coincides with N_l only for an incompressible blend model. Figure 1 displays examples of monomer structures used in our calculations. The submonomer units lie on single lattice sites and are joined by fully flexible bonds. The lattice is assumed to be a three-dimensional cubic lattice with coordination number $z=6$.

Compressibility is introduced into our lattice model by the presence of $n_v=N_l-N_{\rm occ}$ empty sites (voids) to represent excess free volume in the system. The voids permit the system to have variable volume at constant numbers n_1 and n_2 of chains and, therefore, enable the definition of the pressure P, which does not exist for incompressible models. At constant pressure P, temperature T, and number of occupied sites $N_{\rm occ}$, the total number of voids must vary with a blend composition as well as with T and P. The composition of structured monomer compressible blends is expressed below in terms of the nominal volume fractions $\Phi_1=1-\Phi_2\equiv n_1M_1/N_{\rm occ}$, or the actual volume fractions $\phi_\alpha=\Phi_\alpha(1-\phi_v)$, $\alpha=1$ and 2, where $\phi_v\equiv n_v/N_l$ is the void volume fraction and $\phi_1+\phi_2+\phi_v=1$.

While short range repulsions are naturally described by excluded volume constraints which prohibit two submonomer units to lie at the same lattice site, the longer range attractive interactions are modeled by a van der Waals energy $\epsilon_{\alpha\beta}$ between any two nearest neighbor submonomer units i and j of polymer species α and β. For simplicity, we employ a single averaged van der Waals energy for all submonomer units of a given monomer. It is possible to introduce specific interactions, i.e., more than three energies ϵ_{ij} for a binary blend, within the lattice cluster theory, and this specific interaction extension is currently being developed.[24]

B. Gibbs free energy of binary blend

The lattice cluster theory (LCT) has been described extensively in our previous papers.[25–28] The Helmholtz free energy F of a binary blend is a basic quantity that is derived from this theory in the form

$$\frac{F(\phi_1,\phi_v,T,N_l)}{N_lk_BT}=\phi_v\ln\phi_v+\sum_{i=1}^{i=2}\frac{\phi_i}{M_i}\ln\frac{2\phi_i}{M_i}-(\ln z-1)\times\sum_{i=1}^{i=2}\left(1-\frac{1}{M_i}\right)\phi_i+\sum_{m=1}^{m^*}\sum_{n=0}^{m}f_{mn}\phi_1^n\phi_2^{m-n},\tag{2.1}$$

where the last term on the right hand side of Eq. (2.1) represents the noncombinatorial part of F. The coefficients f_{mn} in Eq. (2.1) are obtained from the LCT as double expansions in the inverse lattice coordination number $1/z$ and in the three dimensionless microscopic van der Waals attractive energies $\epsilon_{\alpha\beta}/k_BT$. The coefficients in these double expansions depend on the monomer structures of the two blend components and on the site occupancy indices M_α. The present computations retain only terms through orders $1/z^2$ and $(\epsilon_{\alpha\beta}/k_BT)^2$ in the double summation over m and n in Eq. (2.1). This restricts[26,27] the upper limit of m to $m^*=6$.

The experiments of interest are performed at constant pressure. Thus, the appropriate thermodynamic potential is the Gibbs free energy G which is related to F by the well-known formula

$$G=F+PV=F+PNa_{\rm cell}^3,\tag{2.2}$$

where the pressure P is computed as

$$P\equiv-\left.\frac{\partial F}{\partial V}\right|_{T,n_1,n_2}=-\frac{1}{a_{\rm cell}^3}\left.\frac{\partial F}{\partial n_v}\right|_{T,n_1,n_2}=-\frac{1-\phi_v}{a_{\rm cell}^3N_l}\left.\frac{\partial F}{\partial\phi_v}\right|_{T,n_1,n_2}.\tag{2.3}$$

Equations (2.2) and (2.3) treat the volume $v_{\rm cell}=a_{\rm cell}^3=V/N_l$ associated with one lattice site as a constant and this parameter is estimated from the molar monomer volumes v_α as

$$a_{\text{cell}}^3=\frac{(v_1v_2)^{1/2}}{(s_1s_2)^{1/2}N_{\text{Av}}}, \tag{2.4}$$

with N_{Av} Avogadro's number. The equation of state from Eq. (2.3) is used to determine ϕ_v as a function of thermodynamic state, i.e., as a function of Φ_1, T, and P.

C. Conditions for stability, coexisting phases, and critical point

A binary polymer blend at constant pressure P and temperature T is stable (or metastable) if

$$\left.\frac{\partial^2 g}{\partial\Phi_1^2}\right|_{P,T}>0, \tag{2.5a}$$

where g is the specific Gibbs free energy. Since the composition is specified by the nominal volume fraction

$$\Phi\equiv\Phi_1=\frac{n_1M_1a_{\text{cell}}^3}{N_{\text{occ}}a_{\text{cell}}^3}, \tag{2.6a}$$

the free energy g must be expressed per unit occupied volume (or per occupied lattice site)[29]

$$g\equiv\frac{G}{N_{\text{occ}}a_{\text{cell}}^3}. \tag{2.6b}$$

Equating the left-hand side of Eq. (2.5a) to zero produces the condition for the constant pressure spinodal as

$$\left.\frac{\partial^2 g}{\partial\Phi^2}\right|_{P,T}=0. \tag{2.5b}$$

Calculations of the derivative (2.5b) are facilitated by conversion to the equivalent, but more convenient form

$$\left.\frac{\partial\mu_1^*}{\partial\Phi}\right|_{P,T}-\left.\frac{\partial\mu_2^*}{\partial\Phi}\right|_{P,T}=0, \tag{2.7a}$$

by using the well-known identity

$$dG=\mu_1^*M_1dn_1+\mu_2^*M_2dn_2=M_1(\mu_1^*-\mu_2^*)dn_1,\quad P,T,N_{\text{occ}}=\text{const}, \tag{2.7b}$$

where μ_α^* is the chemical potential of polymer species α (on a per lattice site basis) defined as

$$\mu_\alpha^*(\phi_v,\Phi,T)=\left.\frac{1}{M_\alpha}\frac{\partial F}{\partial n_\alpha}\right|_{n_\beta,V,T}=\left.\frac{\partial[F/(N_lk_BT)]}{\partial\phi_\alpha}\right|_{\phi_\beta,N_l,T}, \tag{2.8a}$$

$$=\left.\frac{1}{M_\alpha}\frac{\partial G}{\partial n_\alpha}\right|_{n_\beta,P,T}. \tag{2.8b}$$

The constant pressure derivatives in (2.7a) are evaluated using standard chain rule relations

$$\left.\frac{\partial\mu_\alpha^*}{\partial\Phi}\right|_{P,T}=\left.\frac{\partial\mu_\alpha^*}{\partial\Phi}\right|_{\phi_v,T}+\left.\frac{\partial\mu_\alpha^*}{\partial\phi_v}\right|_{\Phi,T}\left.\frac{\partial\phi_v}{\partial\Phi}\right|_{P,T}, \tag{2.9}$$

while the derivative $(\partial\phi_v/\partial\Phi)_{P,T}$ is naturally found by differentiating the equation of state (2.3)

$$\left.\frac{\partial\phi_v}{\partial\Phi}\right|_{P,T}=-\left.\frac{\partial P}{\partial\Phi}\right|_{\phi_v,T}\Big/\left.\frac{\partial P}{\partial\phi_v}\right|_{\Phi,T}. \tag{2.10}$$

Thus, expressions (2.1), (2.3), 2.5(b), (2.7a), and (2.8a) enable computation of the constant pressure LCT spinodal curve.

When phase separation occurs at constant pressure P, the coexisting phases (designated as I and II) have equal pressures and equal chemical potentials for both polymer species

$$\mu_\alpha^{*(\text{I})}=\mu_\alpha^{*(\text{II})},\quad \alpha=1 \text{ and } 2, \tag{2.11}$$

$$P^{(\text{I})}=P,\quad P^{(\text{II})}=P. \tag{2.12}$$

The spinodal and coexistence curves coincide at the critical point, where the third derivative of g with respect to Φ also vanishes

$$\left.\frac{\partial^3 g}{\partial\Phi^3}\right|_{P,T=T_c}=0. \tag{2.13}$$

Conditions (2.5b) and (2.13) permit the determination of the critical composition and critical temperature. Equation (2.13) is equivalent to the relation

$$\left.\frac{\partial^2\mu_1^*}{\partial\Phi^2}\right|_{P,T=T_c}-\left.\frac{\partial^2\mu_2^*}{\partial\Phi^2}\right|_{P,T=T_c}=0, \tag{2.14}$$

The second derivatives of the chemical potentials in Eq. (2.14) may then be obtained by twice differentiating μ_α^* according to Eq. (2.9), giving

$$\left.\frac{\partial^2\mu_\alpha^*}{\partial\Phi^2}\right|_{P,T}=\left.\frac{\partial^2\mu_\alpha^*}{\partial\Phi^2}\right|_{\phi_v,T}+2\left.\frac{\partial^2\mu_\alpha^*}{\partial\Phi\partial\phi_v}\right|_{T}\left.\frac{\partial\phi_v}{\partial\Phi}\right|_{P,T}+\left.\frac{\partial^2\mu_\alpha^*}{\partial\phi_v^2}\right|_{\Phi,T}\left(\left.\frac{\partial\phi_v}{\partial\Phi}\right|_{P,T}\right)^2+\left.\frac{\partial\mu_\alpha^*}{\partial\phi_v}\right|_{\Phi,T}\left.\frac{\partial^2\phi_v}{\partial\Phi^2}\right|_{P,T}. \tag{2.15}$$

The second derivative $(\partial^2\phi_v/\partial\Phi^2)_{P,T}$ in Eq. (2.15) is calculated by differentiation of Eq. (2.10) as

$$\left.\frac{\partial^2\phi_v}{\partial\Phi^2}\right|_{P,T}=-\{[(\partial^2P/\partial\Phi^2)_{\phi_v,T}+(\partial^2P/\partial\Phi\,\partial\phi_v)_T(\partial\phi_v/\partial\Phi)_{P,T}](\partial P/\partial\phi_v)_{\Phi,T}-[(\partial^2P/\partial\Phi\,\partial\phi_v)_T$$
$$+(\partial^2P/\partial\phi_v^2)_{\Phi,T}(\partial\phi_v/\partial\Phi)_{P,T}](\partial P/\partial\Phi)_{\phi_v,T}\}/\{[(\partial P/\partial\phi_v)_{\Phi,T}]^2\}. \tag{2.16}$$

All necessary derivatives may be derived analytically from Eq. (2.1), but the formulas are too lengthy to be presented here.

III. GINZBURG CRITERION FOR POLYMER BLENDS AT CONSTANT PRESSURE

Consider a homogeneous binary blend. The formal expansion of the specific Gibbs free energy g around the critical point has the form

$$\frac{g}{k_BT}=\frac{g_0}{k_BT_c}+a_0\eta+\frac{1}{2}a\eta^2\tau+\frac{1}{3!}a_1\eta^3\tau+\frac{1}{4!}b\eta^4+\cdots. \tag{3.1}$$

Equation (3.1) presumes that the specific Gibbs free energy g is an analytic function of η and τ, where the order parameter η is defined as the difference $\eta\equiv\Phi-\Phi_c(P)$ [$\Phi_c(P)$ is the critical composition at pressure P] and $\tau\equiv[T-T_c(P)]/T$ is the reduced temperature, while the coefficients

$$a\equiv\frac{\partial^3(g/k_BT)}{\partial\eta^2\partial\tau} \tag{3.2}$$

and

$$b\equiv\frac{\partial^4(g/k_BT)}{\partial\eta^4} \tag{3.3}$$

are the Gibbs free energy derivatives evaluated at the constant pressure critical point (i.e., at $\Phi=\Phi_c$ and $T=T_c$). Blends with an upper critical solution temperature exhibit $a>0$, while blends with a lower critical temperature have $a<0$. Thermodynamic stability imposes[5,15] the constraint $b>0$. The high molecular weight limit of the FH theory predicts $b(N_1,N_2\to\infty)\to0$, but this is not necessarily the case in the lattice cluster theory and real systems. It should be emphasized that the vanishing of b can have important implications on phase separation critical behavior even within a mean-field theory.[30] The form (3.1) differs from Landau expansions[5] for ferromagnetic systems by the presence of odd powers of η that cannot be removed by an order parameter transformation. The coefficients $a_0\equiv\partial(g/k_BT)/\partial\eta$, $a_1\equiv\partial^4(g/k_BT)/\partial\eta^3\partial\tau$, etc., do not generally vanish at the critical points of binary liquids. The latter only influences[31] the asymmetry of the phase diagram.

A. Fluctuations in compressible system

The simplest way to append contributions from fluctuations of the order parameter involves the addition of a square gradient term[32] to Eq. (3.1). This converts Eq. (3.1) into the free energy functional expansion

$$\frac{g}{k_BT}=\frac{g_0}{k_BT_c}+a_0\eta+\frac{1}{2}a\eta^2\tau+\frac{1}{3!}a_1\eta^3\tau+\frac{1}{4!}b\eta^4$$
$$+\frac{1}{2}\frac{c_0}{a_{\text{cell}}^3}|\nabla\eta|^2+\cdots, \tag{3.4}$$

where the order parameter $\eta=\eta(\mathbf{r})$ is now allowed to be spatially varying. The square gradient coefficient c_0 in Eq. (3.4) must be evaluated at the critical point, i.e., $c_0=c(\Phi=\Phi_c,\ T=T_c)$.

The standard incompressible blend random phase approximation (RPA) estimates c as

$$c^{(\text{inc})}=\frac{1}{18}\left[\frac{l_1^2}{s_1\Phi}+\frac{l_2^2}{s_2(1-\Phi)}\right], \tag{3.5}$$

where l_α is the Kuhn length for monomers of species α. However, Eq. (3.5) neglects the influence of blend compressibility. This deficiency is eliminated in the recent Tang–Freed gradient expansion[17] for the Helmholtz free energy functional of binary blends. The gradient expansion[17] contains contributions from the independent fluctuations $(\nabla\phi_1)^2$ and $(\nabla\phi_2)^2$. At constant pressure, these gradients may be transformed into composition fluctuation contributions from $(\nabla\Phi)^2$, leading to the generalization of Eq. (3.5) as

$$c=\frac{1}{18}\left[\frac{l_1^2}{s_1\Phi}\left(1-\frac{\Phi}{1-\phi_v}\left.\frac{\partial\phi_v}{\partial\Phi}\right|_{P,T}\right)^2\right.$$
$$\left.+\frac{l_2^2}{s_2(1-\Phi)}\left(1+\frac{1-\Phi}{1-\phi_v}\left.\frac{\partial\phi_v}{\partial\Phi}\right|_{P,T}\right)^2\right]. \tag{3.6}$$

The volume fraction ϕ_v and the derivative $(\partial\phi_v/\partial\Phi)_{P,T}$ in Eq. (3.6) are determined from the equation of state (2.3) as described in Eq. (2.10). Equation (3.6) is also a generalization of Eq. (24c) from[15] paper II to polymer blends with monomer structures.

The coefficient c_0 is also related to the correlation length defined as

$$S(q)=\frac{S(0)}{1+q^2\xi^2},\quad q\to0 \tag{3.7}$$

by (see Ref. 32)

$$c_0=\frac{\xi^2(\Phi_c,|\tau|\geqslant0)}{\chi_{\text{MF}}(\Phi_c,|\tau|\geqslant0)}, \tag{3.8}$$

where χ_{MF} is the mean field susceptibility obtained from Eq. (3.1) as

$$\chi_{\text{MF}}^{-1}=v_{\text{cell}}\left.\frac{\partial^2(g/k_BT)}{\partial\Phi^2}\right|_{P,T}. \tag{3.9}$$

The structure factor $S(q)$ in Eq. (3.17) is for pure composition fluctuations in the long wavelength limit, and $S(0)$ corresponds to its value for $q=0$. At the critical point, both the correlation length and susceptibility diverge asymptotically as

$$\chi_{\mathrm{MF}}(\Phi_c,|\tau|\geqslant 0)=(v_{\mathrm{cell}}a\tau)^{-1}, \tag{3.10}$$

$$\xi(\Phi_c,|\tau|\geqslant 0)=\xi_0(\Phi_c)\,|\tau|^{-1/2}, \tag{3.11}$$

thereby giving

$$c_0=v_{\mathrm{cell}}|a|\xi_0^2(\Phi_c). \tag{3.12}$$

The prefactor $\xi_0(\Phi_c)$ is called the correlation length amplitude. An incompressible theory treats χ_{MF} and $S(0)$ interchangeably and this transforms Eq. (3.8) into the widely used formula

$$c=\frac{\xi^2}{S(0)}. \tag{3.13}$$

However, for compressible blends, c_0 calculated from Eq. (3.8) is expected to differ somewhat from $c_0=c(\Phi_c,T_c)$ of Eq. (3.13) due to equation of state effects, etc. [c_0 from Eq. (3.8) is the same as that produced by Eq. (3.6) when ξ is determined[33] from the compressible RPA and LCT.] Generally, experimental data involve scattering only from component 1, and $S(0)$ in Eq. (3.13) is replaced by the partial structure factor $S_{11}(0)$, which need not be identical in a compressible system where fluctuations of component 1 may involve both density and composition fluctuations. Our LCT computations for PS(D)/PVME and PS(D)/PMMA blends show that the difference between these two c_0's from Eqs. (3.8) and (3.13) does not exceed 40% and diminishes quickly with a decrease of the critical temperature.

B. Ginzburg criterion

Different derivations exist for the Ginzburg criterion, which estimates the range of temperature in which mean field theory is applicable. For example, a Ginzburg criterion can be derived from Eq. (3.4) by assuming that classical behavior is valid when the fluctuation correction $\chi_{\mathrm{corr}}^{-1}$ to the inverse susceptibility $\chi^{-1}(\Phi_c)$ remains small compared to the mean field susceptibility $\chi_{\mathrm{MF}}^{-1}(\Phi_c)=v_{\mathrm{cell}}a\tau$ of Eq. (3.10). As shown in Ref. 32 and our forthcoming paper,[15] this assumption leads to the classical regime applying when the inequality

$$|\tau|\geqslant\frac{b^2}{64\pi^2|a|\,(c_0/v_{\mathrm{cell}})^3} \tag{3.14}$$

is satisfied, where a and b are the Gibbs free energy derivatives defined by Eqs. (3.2) and (3.3), and $c_0=c(\Phi_c,T_c)$ is the square gradient term coefficient of Eq. (3.6) that is evaluated at the critical point. The inequality (3.14) is appriopriate for states of the system lying in the one phase region, although this criterion can be immediately generalized to the two phase region,[15,32,34] where a different numerical prefactor appears in Eq. (3.14). (The critical regime is narrower when approached from the two phase region.[15]) The right-hand side of Eq. (3.14) defines the Ginzburg number Gi as

$$\mathrm{Gi}\equiv\frac{b^2}{64\pi^2|a|\,(c_0/v_{\mathrm{cell}})^3}=\frac{b^2}{64\pi^2a^4\xi_0^6}. \tag{3.15}$$

Condition (3.14) for the classical one phase region may then be rewritten as

$$|\tau|\gg\mathrm{Gi}. \tag{3.16}$$

The inverse susceptibility $\chi^{-1}(\Phi_c,|\tau|\geqslant 0)$ is expressed in terms of the Ginzburg number as[32]

$$\begin{aligned}\chi^{-1}(\Phi_c,|\tau|\geqslant 0)&=\chi_{\mathrm{MF}}^{-1}+\chi_{\mathrm{corr}}^{-1}\\&=v_{\mathrm{cell}}a\tau\left[1-\left(\frac{\mathrm{Gi}}{|\tau|}\right)^{1/2}+O(|\tau|^{-1})\right].\end{aligned} \tag{3.17}$$

Other derivations[5,15,32] define Ginzburg numbers with somewhat different numerical prefactors than in Eq. (3.15). This is natural given that different properties exhibit deviations from mean field theory at different temperatures. The present paper uses the definition (3.15) because it is most appropriate for describing scattering data and is less restrictive than other formulas.[5,15,32]

Because the Ginzburg criterion (3.15) involves a strong inequality, the criterion provides[32] only a rough guide to where mean field theory breaks down. Thus, the condition $\tau\approx\mathrm{Gi}$ only identifies the center of a broad crossover regime separating the temperature range where mean field theory is applicable ($\tau>\tau_{\mathrm{MF}}$), and the range where power law critical behavior is exhibited ($\tau<\tau_{\mathrm{crit}}$). Hence, the expected relation is $\tau_{\mathrm{MF}}>\mathrm{Gi}>\tau_{\mathrm{crit}}$. Renormalization group theory allows a more precise delineation of the temperature $\tau=\tau_{\mathrm{MF}}$ at which mean field theory breaks down and the temperature $\tau=\tau_{\mathrm{crit}}$ at which asymptotic critical behavior begins to be exhibited. A direct comparison of $\chi(\Phi_c,|\tau|\geqslant 0)$ with Φ^4 field theory leads again to the expansion (3.17). The expansion in Eq. (3.17) is well known and is recently discussed by Belyakov and Kiselev.[35] More general calculations have been given by Wang *et al.*[36] for the $O(m)$ model, where $m\to 1$ corresponds to the Ising model studied by Belyakov and Kiselev[35] and $m\to 0$ corresponds to polymers in dilute solution. Crossover for a broad class of phase transitions may thus be discussed in a unified way.

Renormalization group theory describes the full crossover dependence of $\chi(\Phi_c,|\tau|\geqslant 0)$ among three regimes—a weak coupling regime, where mean field theory is a good approximation; a crossover regime, where critical fluctuations are large enough to spoil the mean field description, but insufficiently strong to exhibit asymptotic scaling critical behavior; and finally the asymptotic strong coupling regime, where scaling behavior is exhibited. These regimes have been described in detail by using the renormalization group methods for dilute polymer solutions, where the Fixman excluded volume parameter z_2 is the direct analog of the dimensionless interaction $(\mathrm{Gi}/|\tau|)^{1/2}$ in Eq. (3.17) (see Wang *et al.*[36]). A direct generalization of previous

calculations for these different regimes of crossover in a polymer solution context[37,38] to the cross-over description of critical fluids leads in three spacial dimensions to a specification of the different regimes

$$\tau \geqslant \tau_{MF} \approx 10\ \mathrm{Gi} \quad \text{(mean field regime)}, \tag{3.18a}$$

$$\tau \leqslant \tau_{crit} \approx \mathrm{Gi}/10 \quad \text{(critical regime)}, \tag{3.18b}$$

$$\tau_{MF} > \tau > \tau_{crit} \quad \text{(crossover regime)}. \tag{3.18c}$$

The classification in Eqs. (3.18a)–(3.18c) is presented by analogy with theories for dilute solution of flexible polymers, where these three regimes correspond to the poor, good, and marginal solvents.[38] Specifically, these regimes are defined for polymers in terms of the Fixman parameter z_2 as $(d=3)$,

$$z \leqslant u_2^* \quad \text{(poor solvent)}, \tag{3.18d}$$

$$z \geqslant 1 \quad \text{(good solvent)}, \tag{3.18e}$$

$$u_2^* < z < 1 \quad \text{(marginal solvent)}, \tag{3.18f}$$

where the renormalization group fixed point $u_2^*(m \to 0)$ is about 1/5. The Ising analog $(m \to 1)$ in Eqs. (3.18a)–(3.18c) involves a dimensionless scaling variable analogous to z_2, and the renormalization group fixed point has a slightly different value. However, the criteria are mathematically identical. Polymer solutions provide a good system for studying cross-over phenomena because of the high quality data available in the cross-over regime and the ability to vary the coupling constant by a change of both temperature and molecular weight. The mean field theory in this instance corresponds to the experimentally accessible theta region.

The conditions in Eq. (3.18) indicate that the conventional Ginzburg esimate $\tau \approx \mathrm{Gi}$ yields a temperature lying roughly in the middle of the rather broad cross-over regime as expected. The significance of the cross-over estimates in Eq. (3.18) can be appreciated from a systematic examination[39] of τ_{crit} for a variety of liquid–liquid and liquid–vapor phase transitions. A variety of small molecule (nonquantum) liquids have τ_{crit} on the order of 10^{-3} in the one phase region, while Gi estimated[32] from the van der Waals theory is $O(10^{-2})$. Thus, Eq. (3.18b) provides good order of magnitude consistency between experiment and the van der Waals theory estimate of Gi for small molecule liquids. Preliminary evidence[40] indicates that τ_{MF} in small molecule fluids should be somewhat larger than 10Gi, so that even Eq. (3.18a) should be interpreted as a rough order of magnitude criterion because experimental estimates apply different analyses than those used to produce Eqs. (3.18a) and (3.18b). This brief discussion clearly indicates that the criterion $\tau \approx \mathrm{Gi}$ provides a gross overestimate of the temperature where mean field theory breaks down.

C. Semiempirical treatments of the Ginzburg criterion

All prior analyses of the Ginzburg criterion are based on the use of incompressible FH theory (with composition independent χ_{eff} parameter) and most employ the incompressible RPA. Real polymer blends, however, have liquid-like compressibility and generally exhibit composition dependent interaction parameters. The recent analysis of Hobbie *et al.*[41] for polystyrene/polybutadiene blends attempts to overcome some of the deficiencies of FH and RPA theories by introducing directly observable quantities into the Ginzburg number definition (3.15). This treatment involves estimation of the two basic quantities a and c_0 in Gi from experimental data for the critical composition. However, the available data are generally obtained far from the critical temperature, despite the fact that both a and c_0 are defined in Eq. (3.15) as being evaluated at the critical point. Likewise, the data often are not at the critical composition because of the difficulty in precisely determining Φ_c. Important questions therefore arise as to the accuracy of the necessary extrapolation or interpolation of available experimental data to find a and c_0.

The derivative a is obtained by extrapolating the experimental structure factor $S(0,\Phi_c)$ using the assumed form

$$S(0,\Phi_c)^{-1} \approx v_m a \tau,$$

where v_m is the average monomer volume. Alternatively, a is determined from incompressible FH theory with χ_{eff}^{ent} extracted from experimental data for $\chi_{eff}(\Phi_c,T)$ [see Eq. (4.2) below]. The square gradient coefficient c_0 is calculated from Eq. (3.12), where the correlation length amplitude $\xi_0(\Phi_c)$ is found from a temperature fit to the experimental correlation lengths $\xi(\Phi_c,T)$ by using Eq. (3.11). It is, however, unclear to what extent the use of experimental data far from the critical temperature and somewhat off the critical composition accurately reflects the critical point thermodynamic derivative a and the correlation length amplitude ξ_0. In this context, the compressible LCT provides an estimation of possible errors associated with such extrapolations because the LCT is more realistic than the FH theory for performing these extrapolations. Unlike a and c_0, the derivative b cannot be obtained from experimental scattering data and is evaluated using incompressible FH theory as $b=[N_1^{-1}\Phi_c^{-3}+N_2^{-1}(1-\Phi_c)^{-3}]/v_m$. Hair *et al.*[11] and Hobbie *et al.*[41] use the experimental critical composition in this formula for b since the FH theory prediction for Φ_c is often totally wrong (see Sec. IV for more detail).

The computations of the Ginzburg number in Sec. IV below employ the LCT and thereby allow us to determine the influence of "equation of state effects," local correlations, and monomer structure upon the size of the nonclassical region. This enables the first treatment of the pressure dependence of Gi and a test of using data far from T_c to evaluate Gi. Section IV also provides illustrations of discrepancies between predictions of the more realistic LCT and prior zeroth order theories that are based on incompressible FH theory.

IV. COMPUTATIONS OF GINZBURG NUMBERS FOR PS/PVME AND PS/PMMA BLENDS

This section summarizes calculations of the Ginzburg number for PS/PVME and PS/PMMA binary blends by using theoretical developments described in Secs. II and III. The PS/PVME blend is modeled by a mixture of

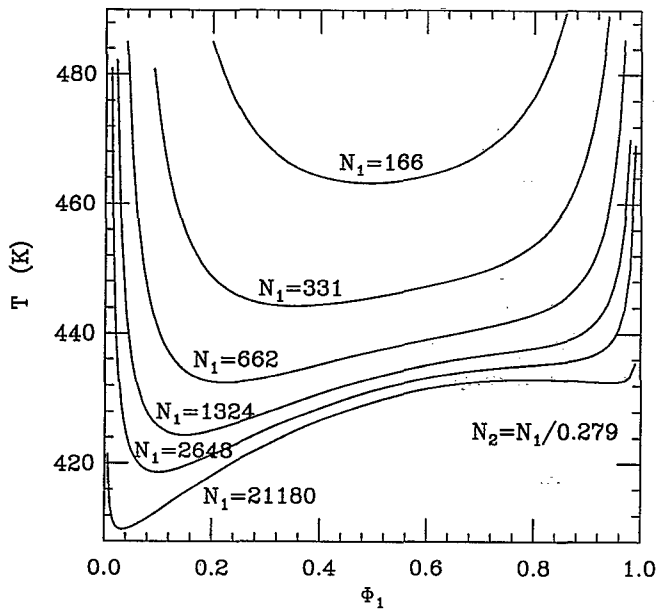

FIG. 2. Lattice cluster theory spinodal curves for PS/PVME blends at $P=1.013\times10^5$ Pa. The microscopic attractive van der Waals energies are taken from our previous fits (Ref. 14) as $\epsilon_{S\text{-}S}=0.5k_BT_0$, $\epsilon_{VME\text{-}VME}=0.56k_BT_0$, and $\epsilon_{S\text{-}VME}=0.533\,605k_BT_0$ ($T_0=415.15$ K). All subsequent figures for PS/PVME blends use the same $\{\epsilon_{\alpha\beta}\}$ and the fixed ratio of polymerization indices $N_{PS}/N_{PVME}=0.279$. Component 1 is always PS.

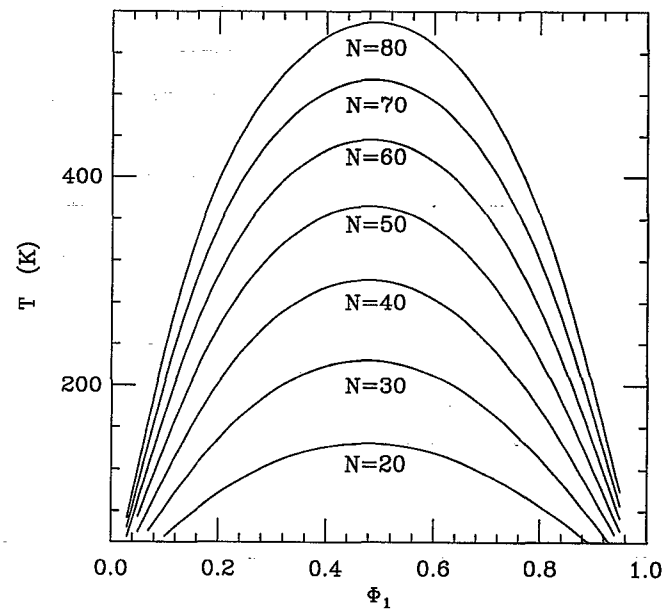

FIG. 3. Lattice cluster theory spinodal curves for PS/PMMA blends at $P=1.013\times10^5$ Pa. The attractive van der Waals energies are taken from our previous fit (Ref. 19) for a PS-*b*-PMMA diblock melt as $\epsilon_{S\text{-}S}=0.5k_BT_0$, $\epsilon_{MMA\text{-}MMA}=0.4753k_BT_0$, and $\epsilon_{S\text{-}MMA}=0.486\,445k_BT_0$ ($T_0=415.15$ K). All subsequent figures for PS/PMMA blends use the same $\{\epsilon_{\alpha\beta}\}$ and polymerization indices $N_{PS}=N_{PMMA}=N$. Component 1 is always PS.

chains constructed from monomers with structures 1(b) and 1(a), while the PS/PMMA binary system is represented by polymer chains composed of monomers with structures 1(b) and 1(c). Each of the circles in Fig. 1 occupies a single lattice site and the lines represent flexible bonds. These two particular polymer blends are chosen because the microscopic van der Waals attractive energies $\{\epsilon_{\alpha\beta}\}$ have been obtained from fits[14,19] of the LCT predictions to experimental neutron scattering and thermodynamic data.[20–22] The above energetic parameters are used within the LCT to evaluate a, b, and c at the critical point. Based on previous comparisons[14,33] with experiment, the lattice cluster theory is a superior theory for extrapolating–interpolating experimental data to the critical point. It should, however, be noted that the fits[19] for the PS/PMMA system come from very limited data[22] for a PS-*b*-PMMA diblock copolymer melt. The block copolymer energetic parameters ($\epsilon_{\alpha\beta}$) are taken as transferable to the corresponding binary blend. Thus, the PS-*b*-PMMA parameters are of more limited reliability.

A. LCT computations of phase diagrams and critical parameters

The two blends are also chosen because they exhibit very different phase diagrams. The PS/PVME blend has a lower critical solution temperature whose physical origin is understood by use of a compressible theory.[16] On the other hand, the PS/PMMA blend displays an upper critical solution temperature. The computed spinodal curves for these two systems (using the energetic parameters from Refs. 14 and 19, respectively) are illustrated in Figs. 2 and 3. Figure 2 depicts the spinodal curves for PS/PVME blends at $P=1.013\times10^5$ Pa for different polymerization indices N_1 and N_2 with the fixed ratio $N_1/N_2=0.279$. The sample with $N_1=5295$ and $N_2=N_1/0.279=18\,965$ has been used by Han *et al.*[20] in small-angle neutron scattering (SANS) experiments and by us in LCT fits[14] to their data. The PS/PVME phase diagram changes from almost a symmetrical form (with a flat minimum) for low molecular weights to a highly unsymmetrical form (with a sharp minimum) for higher molecular weights. The latter form is reminiscent of phase diagrams for solutions of polymers in small molecule solvents.[23] Both the computed critical temperature and critical composition of the PS/PVME blend depend strongly on molecular weights as is shown in Figs. 4 and 5, respectively. The critical parameters in Figs. 4 and 5 are plotted for a constant ratio $N_1/N_2=0.279$ as a function of $1/N_1$. Except for the region of low molecular weights ($N_1\leqslant662$), the critical temperature T_c scales as $1/N_1^{1/2}$, while the critical composition scales like $1/N^{11/20}$. Figure 5 contrasts profoundly with incompressible FH theory, which predicts the critical composition $\Phi_c^{(inc)}$,

$$\Phi_c^{(inc)}=\frac{N_2^{1/2}}{N_1^{1/2}+N_2^{1/2}} \tag{4.1}$$

to depend only on the ratio of polymerization indices N_1/N_2, which is chosen as constant in our study also to emphasize departures from FH theory predictions. Consequently, the FH critical composition $\Phi_c^{(inc)}$ from Eq. (4.1) is the straight horizontal solid line in Fig. 5. The dashed line is obtained from Eq. (4.1) by replacing the polymerization indices N_α with the site occupancy indices M_α

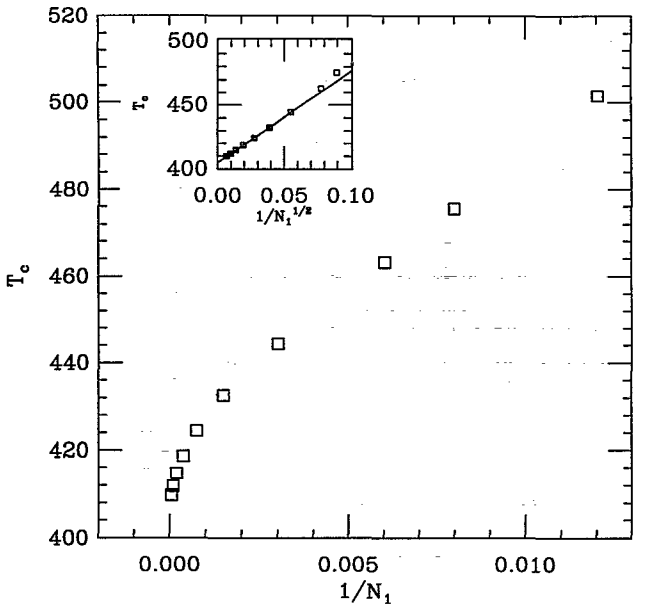

FIG. 4. Lattice cluster theory predictions for molecular weight dependence of the critical temperature T_c for PS/PVME blends at $P=1.013\times10^5$ Pa. The insert shows that T_c scales linearly with $1/N_1^{1/2}$ only for higher molecular weights.

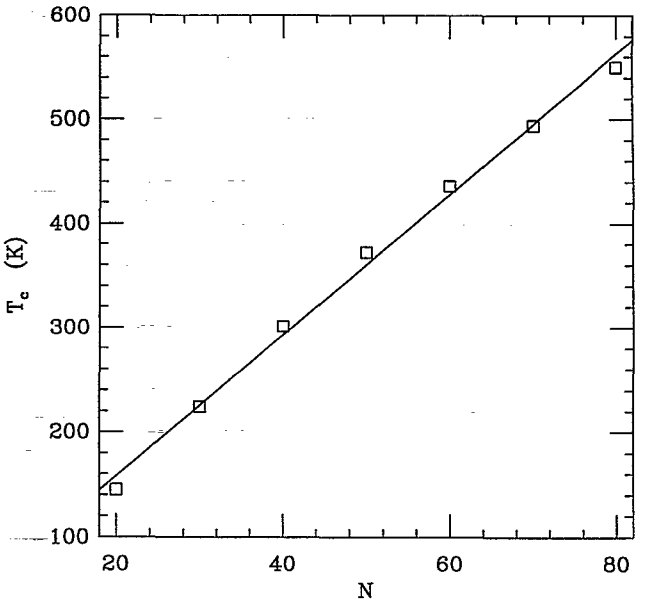

FIG. 6. Lattice cluster theory predictions (squares) for the polymerization index ($N_{PS}=N_{PMMA}=N$) dependence of the critical temperature for PS/PMMS blends at $P=1.013\times10^5$ Pa. The solid line is obtained by a least squares fit.

$=N_\alpha s_\alpha$. The critical composition tends to the FH limit $\Phi_c^{(inc)}$ only for low molecular weights ($N_1<83$).

Phase diagrams for PS/PMMA blends at $P=1.013\times10^5$ Pa are depicted in Fig. 3. Since the polymerization indices N_1 and N_2 for the PS/PMMA samples are taken as identical and the self-interaction energies $\epsilon_{\alpha\alpha}$ ($\alpha=1,2$) are close to each other, the phase diagrams are almost symmetrical. The critical temperature of these nearly symmetrical blends varies linearly with N (see Fig. 6), a trend which agrees with Monte Carlo simulations of Deutsch and Binder,[42] PRISM theory predictions,[43] and recent experiments on isotopic blends by Gehlsen *et al.*[44] The critical composition Φ_c is presented in Fig. 7 as a function of $1/N$ and is compared with incompressible FH theory $\Phi_c^{(inc)}$ (the solid line). The dashed line in Fig. 7 corresponds to an incompressible FH theory estimation of Φ_c when N_i's in Eq. (4.1) are replaced by M_i. The LCT crit-

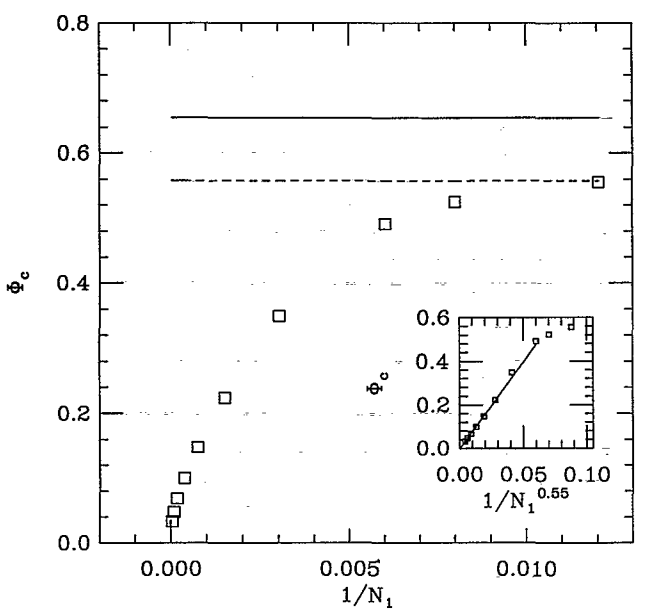

FIG. 5. Lattice cluster theory predictions (squares) for the polymerization index (N_{PS}) dependence of the critical composition Φ_c for PS/PVME blends at $P=1.013\times10^5$ Pa. The solid line corresponds to the incompressible FH estimate (4.1), while the dashed line presents Φ_c when the polymerization indices N_α in Eq. (4.1) are replaced by the site occupancy indices M_α. The insert indicates that Φ_c scales linearly with $1/N_1^{0.55}$ only at higher molecular weights.

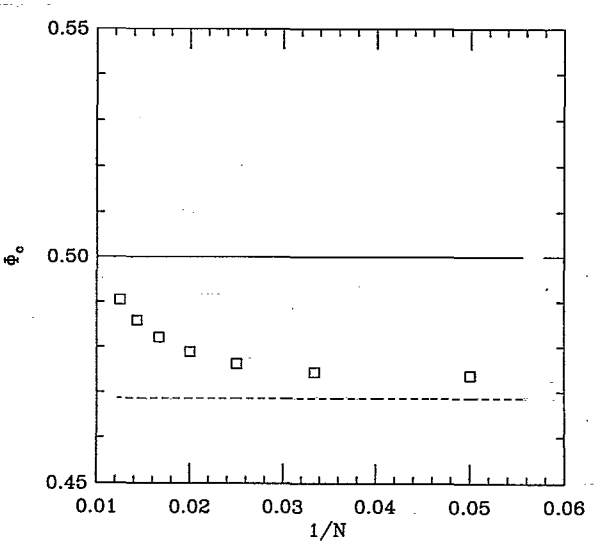

FIG. 7. The same as Fig. 5 for PS/PMMA blends.

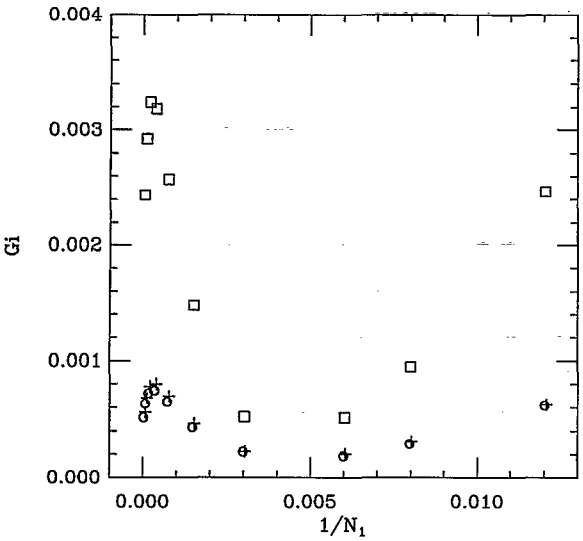

FIG. 8. Lattice cluster theory Ginzburg numbers for PS/PVME blends at $P=1.013\times10^5$ Pa as a function of the polymerization index of PS (squares). Crosses designate the incompressible approximation $Gi^{(inc)}$ from Eq. (4.2) with LCT estimates of χ_{eff}^{ent}, Φ_c, and c_0; and circles illustrate the same $Gi^{(inc)}$ calculated from Eq. (4.2), but with the mixed derivative (3.2) estimated from the LCT $S(0,\Phi_c)$ and the relation $S(0,\Phi_c)^{-1}\approx v_{cell}a\tau$.

ical composition Φ_c deviates from $\Phi_c^{(inc)}=0.5$ by no more than 6%, and the difference diminishes for higher molecular weights.

B. The dependence of Ginzburg numbers on molecular weights, pressure, and source of experimental data

Substituting the LCT Gibbs free energy derivatives a and b and the square gradient term coefficient $c_0=c(\Phi=\Phi_c,T=T_c)$ [see Eqs. (3.2), (3.3), and (3.6)] into Eq. (3.15) gives the LCT Ginzburg numbers. Figure 8 presents the computed Ginzburg numbers for PS/PVME blends (with a constant ratio of N_1/N_2) as a function of $1/N_1$. The squares in Fig. 8 designate the LCT Ginzburg numbers obtained from Eqs. (3.2), (3.3), (3.6), and (3.15), while the crosses correspond to the predictions based (see below) on the Hair *et al.* formula[11]

$$Gi^{(inc)}=\frac{v_m^2[N_1^{-1}\Phi_c^{-3}+N_2^{-1}(1-\Phi_c)^{-3}]^2}{64\pi^2[N_1^{-1}\Phi_c^{-1}+N_2^{-1}(1-\Phi_c)^{-1}-2\chi_{eff}^{ent}]c_0^3}. \quad (4.2)$$

Equation (4.2) can be obtained from Eq. (3.15) by replacing a and b by the corresponding derivatives of the incompressible FH Helmholtz free energy. The volume v_m in Eq. (4.2) is the average monomer volume that coincides with the volume associated with one lattice site within the FH theory model in which each monomer can occupy only one lattice site. The main idea of Hair *et al.*[11] is to introduce into Eq. (4.2) directly observable experimental quantities [such as the critical composition Φ_c; the entropic portion of the FH effective interaction parameter χ_{eff}, defined as $\chi_{eff}^{ent}=\chi_{eff}-\text{const}/T$; and the square gradient term coefficient $c_0\approx\xi(\Phi_c)^2/S(0,\Phi_c)$]. The use of experimental quantities partially corrects expression (4.2) for inadequacies of the simple FH theory and the incompressible RPA. Thus, Eq. (4.2) is more general and useful than the formally equivalent (after notational transcriptions) formula of Bates *et al.*,[7] which uses the incompressible RPA equation (3.5) for c and the FH equation (4.1) for Φ_c. It is only in this latter case, where $\chi_{eff}^{ent}=0$ (or χ_{eff}^{ent} scales as N_1^{-1}) and c_0 is determined from Eqs. (3.5) and (4.1), that $Gi^{(inc)}$ is strictly inversely proportional to N_1 (for constant N_1/N_2).

TABLE I. The LCT Ginzburg numbers Gi for PS/PVME blends at pressure $P=1.013\times10^5$ Pa.

N_{PS}	N_{PVME}	Gi
21 180	75 860	2.44×10^{-3}
10 590	37 930	2.92×10^{-3}
5 295	18 965	3.24×10^{-3}
2 648	9 483	3.18×10^{-3}
1 324	4 741	2.57×10^{-3}
662	2 371	1.48×10^{-3}
331	1 185	5.20×10^{-4}
166	593	5.14×10^{-4}
125	445	9.48×10^{-4}
83	297	2.47×10^{-3}

The current lack of experimental data for PS/PVME blends over a wide enough range of molecular weights leads us to use LCT values of Φ_c, χ_{eff}^{ent}, and c_0 in order to study how the Ginzburg number (4.2) scales with polymerization indices. An adequate comparison of $Gi^{(inc)}$ from Eq. (4.2) and the LCT Gi from Eq. (3.15) requires that the polymerization indices N_α in Eq. (4.2) are replaced by site occupancy indices $M_\alpha=N_\alpha s_\alpha$ and that v_m is given by Eq. (2.4). As shown in Fig. 8, Eqs. (3.15) and (4.2) produce qualitatively similar variations of the two Gi definitions with $1/N_1$. The presence of local minima and maxima for Gi in Fig. 8 indicates a large influence of compressibility, local correlations, and monomer structure on Gi. The influence of all these factors on the phase diagrams and critical parameters is displayed in Figs. 2, 4, and 5. Replacing the FH approximation for the mixed derivative $a=[N_1^{-1}\Phi_c^{-1}+N_2^{-1}(1-\Phi_c)^{-1}-2\chi_{eff}^{ent}]/v_m$ in Eq. (4.2) by a found from the relation $S_{11}(0,\Phi_c)^{-1}\approx v_{cell}a\tau$, where $S_{11}(0,\Phi_c)$ is evaluated from the LCT, leads to practically the same $Gi^{(inc)}$ (circles in Fig. 8). Numerical differences between Gi and $Gi^{(inc)}$ emerge mainly from the discrepancy between the LCT and FH b's, and they demonstrate once again the approximate character of FH theory and its inadequancy in calculating Ginzburg number, even when the critical composition is taken from experiment.

The lattice cluster theory does not produce the simple FH $1/N$ scaling behavior of Gi for PS/PVME blends. In order to better understand the origin of the trends illustrated in Fig. 8 and Table I, the three individual contributions a, b, and c_0 to the LCT Ginzburg number are plotted vs $1/N_1$ (for the fixed ratio $N_1/N_2=0.279$) in Figs. 9, 10, and 11, respectively. Figure 9 demonstrates that the LCT mixed derivative a changes with $1/N_1$ rather slowly (not more than 10% in the range of N_1 between 83 and 21 180). Thus, its behavior deviates considerably from the simple FH theory linear dependence. Figures 10 and 11 exhibit

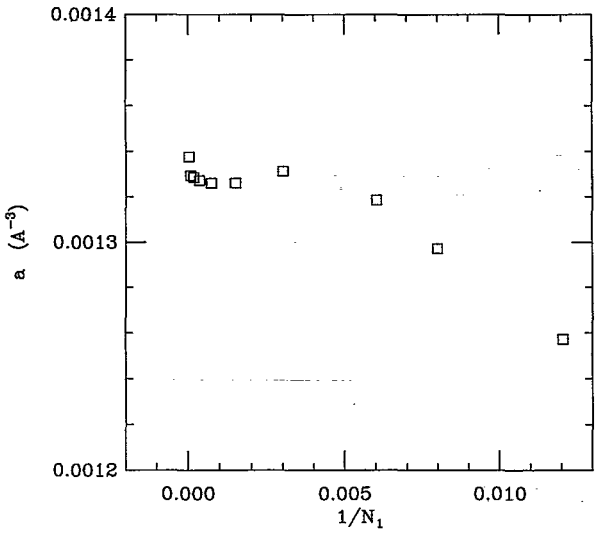

FIG. 9. The LCT Gibbs free energy derivative a of Eq. (3.2) as a function of polymerization index $N_1=N_{PS}$ for PS/PVME blends at $P=1.013\times10^5$ Pa (N_1/N_2=constant).

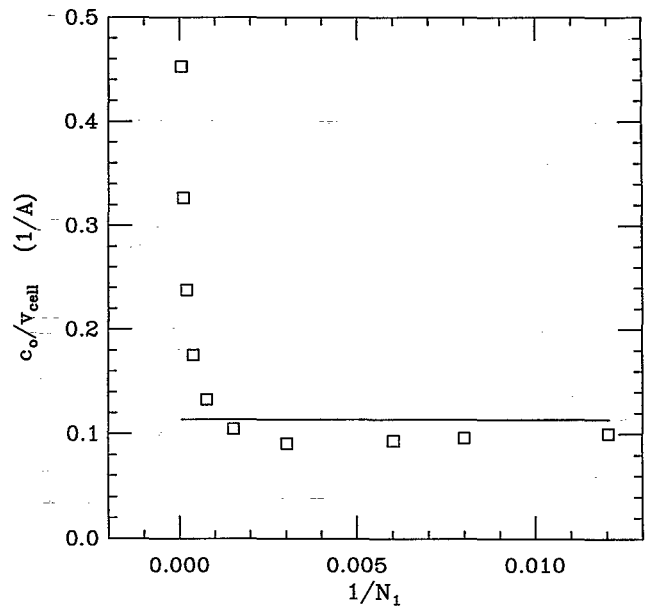

FIG. 11. The square gradient coefficient c_0 as a function of polymerization index $N_1=N_{PS}$ for PS/PVME blends at $P=1.013\times10^5$ Pa (N_1/N_2 =constant).

the significant impact of compressibility, local correlations, and monomer structure on b and c_0 in the high molecular weight region. The LCT Gibbs free energy derivative b (squares in Fig. 10) departs qualitatively from the FH theory predictions (the solid line in Fig. 10) which are commonly used in all prior analysis of the Ginzburg criterion. A similar trend is exhibited by the square gradient term coefficient c_0 in Fig. 11. The low molecular weight range yields only small discrepancies between the c_0's evaluated from the incompressible RPA formula (3.5) (solid line) and from the LCT expression (3.6) (squares). However, the deviations grow rapidly for larger molecular weights. Hence, the LCT nonlinear behavior in $1/N_1$ for all

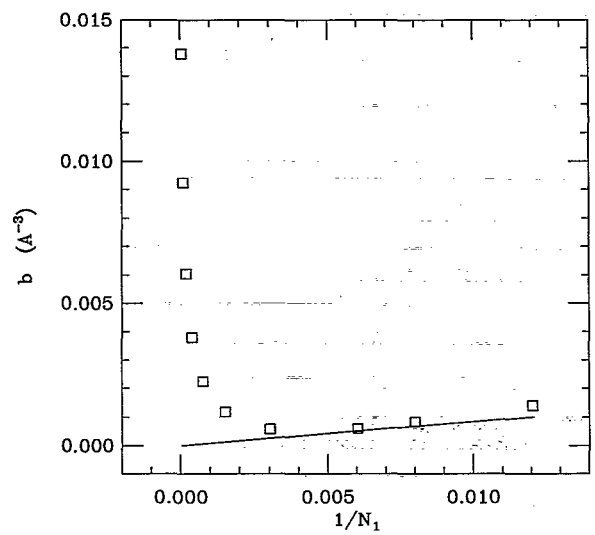

FIG. 10. The LCT Gibbs free energy derivative b of Eq. (3.3) as a function of polymerization index $N_1=N_{PS}$ for PS/PVME blends at $P=1.013\times10^5$ Pa (N_1/N_2=constant). The solid line shows the prediction of incompressible FH theory.

three components of Gi illuminates the non-FH type variation of Gi with $1/N_1$ for PS/PVME blends.

The Ginzburg number and the criterion $|\tau|\gg$Gi provide only an order of magnitude estimate for the range of reduced temperatures τ over which the mean field theory breaks down. The LCT Ginzburg numbers for PS/PVME blends (see Table I and Fig. 8) are of the order of 10^{-3} in the molecular weight range $83\leqslant N_1\leqslant 21\,180$. To determine more precisely the regime of validity for mean field theory, the inverse susceptibility $\chi(\Phi_c)^{-1}$, as well as its mean field contribution χ_{MF}^{-1} and the fluctuation correction χ_{corr}^{-1}, are compared as a function of reduced temperature τ. The mean field region is then defined as that for which the fluctuation correction is small, i.e., for which $\chi_{corr}^{-1}\ll\chi_{MF}^{-1}(\Phi_c)$. Figure 12 displays these quantities for one PS/PVME sample (with $N_1=21\,180$ and $N_2=75\,860$). Both the inverse susceptibility $\chi(\Phi_c)^{-1}$ and the fluctuation correction χ_{corr}^{-1} begin to depart from a linear variation with τ at about $|\tau|=0.02$ which corresponds to $|T-T_c|\approx8.0$ K and which agrees at an order of magnitude level with Eq. (3.18a). The fluctuation correction $\chi_{corr}^{-1}(|\tau|=0.02)$ at this point is, however, about 35% of χ_{MF}^{-1}. When $|\tau|$ lies between 0.05 and 0.02, the contribution of χ_{corr}^{-1} to $\chi_{MF}(\Phi_c)^{-1}$ ranges from 28% to 54%. The example in Fig. 12 demonstrates that a linear variation of $\chi^{-1}(\Phi_c)$ with τ does not imply that contributions from fluctuations are negligible and that mean field theory is totally valid. Moreover, comparing the fluctuation correction χ_{corr}^{-1} with the mean field inverse susceptibility χ_{MF}^{-1}, the nonlinear variation of $\chi^{-1}(\Phi_c)$ with τ first appears in the middle of the cross-over regime. We believe that a similar conclusion applies for $S(0,\Phi_c)$.

The computation of incompressible Ginzburg numbers $Gi^{(inc)}$ from Eq. (4.2) requires a knowledge of experimen-

tal data for $\chi_{\rm eff}^{\rm ent}(\Phi_c,T)$, $\xi(\Phi_c,T)$, and $S(0,\Phi_c,T)$ over a wide temperature range. Such data do not exist even for the three well-studied PS/PVME samples[20] since the experimental compositions are somewhat different from the critical compositions. However, it is useful to examine how the quality of experimental data affects computation of Ginzburg numbers from Eq. (4.2). For PS/PVME blends, the LCT Gi from Eq. (3.15) and $\mathrm{Gi}^{(\rm inc)}$ from Eq. (4.2) are found to be

$$N_1=5295,\quad N_2=18\,965,\quad \mathrm{Gi}(\Phi_c=0.0684)=3.24\times10^{-3},\quad \mathrm{Gi}^{(\rm inc)}(\Phi^{\rm exp}=0.0951)=1.61\times10^{-4},$$

$$N_1=3589,\quad N_2=3621,\quad \mathrm{Gi}(\Phi_c=0.0840)=3.36\times10^{-3},\quad \mathrm{Gi}^{(\rm inc)}(\Phi^{\rm exp}=0.1025)=9.58\times10^{-5},$$

$$N_1=2054,\quad N_2=6707,\quad \mathrm{Gi}(\Phi_c=0.1149)=3.04\times10^{-3},\quad \mathrm{Gi}^{(\rm inc)}(\Phi^{\rm exp}=0.1901)=3.98\times10^{-5},$$

where Φ_c's are evaluated from the LCT, while $\Phi^{\rm exp}$'s are the closest experimental compositions[20] to $\Phi_c^{\rm exp}$. The entropic portion of the effective interaction parameter in Eq. (4.2) is obtained from a linear fit of experimental data[20] for $\chi_{\rm eff}(\Phi^{\rm exp},T)$ vs $1/T$, while the square gradient coeficient c_0 is determined from the experimental correlation lengths[20] $\xi(\Phi^{\rm exp})$ and experimental structure factors[20] $S(0,\Phi^{\rm exp})$ according to Eq. (3.18). The ratio $\xi^2(\Phi^{\rm exp})/S(0,\Phi^{\rm exp})$ is practically constant over a wide temperature range. Not surprisingly, the Ginzburg numbers Gi and $\mathrm{Gi}^{(\rm inc)}$ for a given sample differ by about one or even two orders of magnitude. As mentioned above, this disparity arises because the application of the FH theory to the available experimental data is an inadequate procedure for obtaining the necessary critical point information. The disparity further emphasizes the fact that the effective interaction parameter $\chi_{\rm eff}$ and therefore thermodynamic derivatives at the critical point are very sensitive functions of composition for PS/PVME blends. It is still possible that Eq. (4.2) could be used to obtain an approximate estimate of Ginzburg numbers provided that better experimental data are available (i.e., at the critical compositions), but this is generally a difficult task. If instead we use in Eq. (4.2) the derivative a as determined from the experimental $S(0,\Phi^{\rm exp})$ and $S(0,\Phi^{\rm exp})^{-1}\approx v_m a\tau$, no improvement is found in $\mathrm{Gi}^{(\rm inc)}$,

$$\mathrm{Gi}^{(\rm inc)}(N_1=5295,\ N_2=18\,965,\ \Phi^{\rm exp}=0.0951)=1.53\times10^{-4},$$

$$\mathrm{Gi}^{(\rm inc)}(N_1=3589,\ N_2=3621,\ \Phi^{\rm exp}=0.1025)=9.23\times10^{-5},$$

$$\mathrm{Gi}^{(\rm inc)}(N_1=2054,\ N_2=6707,\ \Phi^{\rm exp}=0.1901)=3.80\times10^{-5},$$

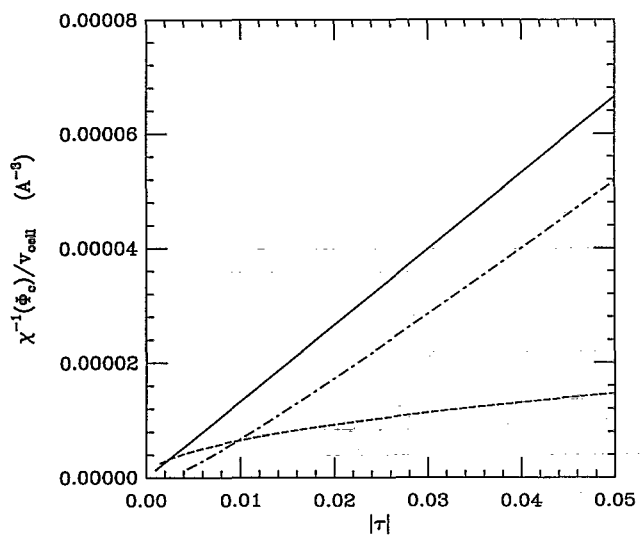

FIG. 12. Lattice cluster theory predictions for the reduced temperature dependence of the inverse susceptibility $\chi^{-1}(\Phi_c)$ (solid line), its mean field contribution $\chi_{\rm MF}^{-1}(\Phi_c)$ (dashed–dotted line), and the fluctuation correction $\chi_{\rm corr}^{-1}$ (dashed line) for a PS/PVME blend ($N_{\rm PS}=21\,180$, $N_{\rm PVME}=75\,860$) at $P=1.013\times10^5$ Pa.

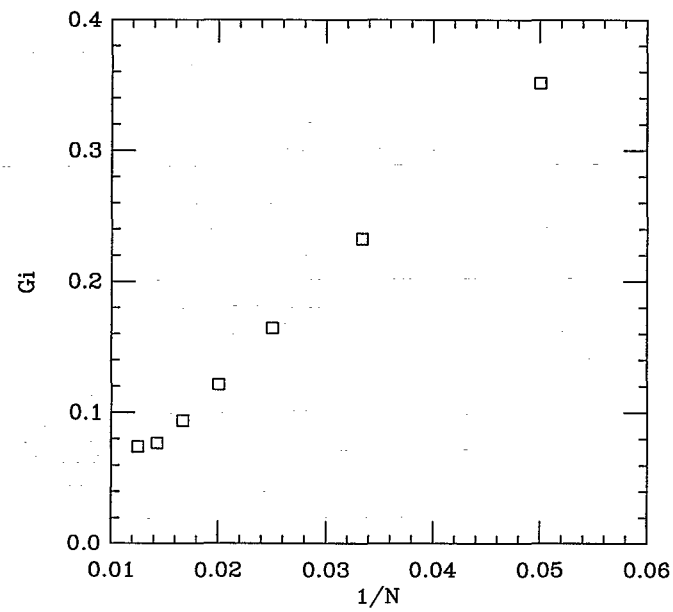

FIG. 13. Lattice cluster theory Ginzburg numbers for PS/PMMA blends at $P=1.013\times10^5$ Pa as a function of polymerization index $N=N_{\rm PS}=N_{\rm PMMA}$.

and there still persists a difference of one or two orders of magnitude between Gi and $Gi^{(inc)}$. We return in Sec. V to the issue of using experimental data in conjuction with Eq. (4.2).

One benefit of using the LCT to compute Gi lies in the ability of taking data further from the critical point in order to fit energetic parameters $\{\epsilon_{\alpha\beta}\}$ and, in turn, to evaluate a, b, and c_0 upon which the Ginzburg number Gi depends. This represents an extrapolation–interpolation of the data with a more realistic mean field approach (the LCT) than the FH theory for describing the critical region.

A much larger extrapolation permits the prediction of the pressure dependence of Ginzburg numbers. LCT computations for PS/PVME blends yield

$P=1.013\times10^5$ Pa	$P=1.013\times10^8$ Pa
$Gi(N_1=21\,180,\ N_2=75\,860)=2.44\times10^{-3}$,	$Gi(N_1=21\,180,\ N_2=75\,860)=3.74\times10^{-3}$,
$Gi(N_1=10\,590,\ N_2=37\,930)=2.92\times10^{-3}$,	$Gi(N_1=10\,590,\ N_2=37\,930)=4.65\times10^{-3}$,.
$Gi(N_1=5295,\ N_2=18\,965)=3.24\times10^{-5}$,	$Gi(N_1=5295,\ N_2=18\,965)=5.47\times10^{-3}$

Thus, an increse in pressure produces a larger Gi and, hence, a larger nonclassical region. However, this trend must be treated with some caution because the attractive interaction energies $\epsilon_{\alpha\beta}$ used in the above computations are taken as pressure independent, whereas the van der Waals energies must become less attractive at higher pressures.

Our previous LCT computations[19] indicate that PS/PMMA blends are homogeneous at temperatures $T>500$ K for low molecular weights. Therefore, only samples with small N ($N=N_1=N_2$) between 20 and 80 are considered in the computations. Figure 13 again exhibits nonlinearity of Gi as a function of $1/N$. Deviations from linearity are more significant in the region of larger polymerization indices $N>60$. The Gibbs free energy derivative b varies linearly with $1/N$ (see Fig. 14, where the dashed line presents the fourth derivative of the incompressible FH Helmholtz free energy with respect to composition). The square gradient coefficient c_0 is illustrated in Fig. 15 and is almost N independent. Therefore, the nonlinear behavior in Fig. 13 comes mainly from the variation of the LCT mixed derivative a that is presented in Fig. 16.

The LCT Ginzburg numbers Gi for PS/PMMA blends seem to be too high to ascribe any physical meaning to them. They are higher by two orders of magnitude than Gi for PS/PVME blends and by one order of magnitude than Gi for small molecule liquids.[32] This discrepancy partially arises from transfering energetic parameters $\epsilon_{\alpha\beta}$ from LCT fits to experimental data for a PS-*b*-PMMA diblock coplymer melt to the corresponding PS/PMMA binary blend. In addition, the data for PS-*b*-PMMA diblock melts are too limited for us to have strong confidence in the LCT fits. Moreover, our LCT fits to the neutron scattering data of Russell[22] are performed for a simplistic diblock copolymer melt model in which the linking group between two blocks is represented by a single bond with a junction

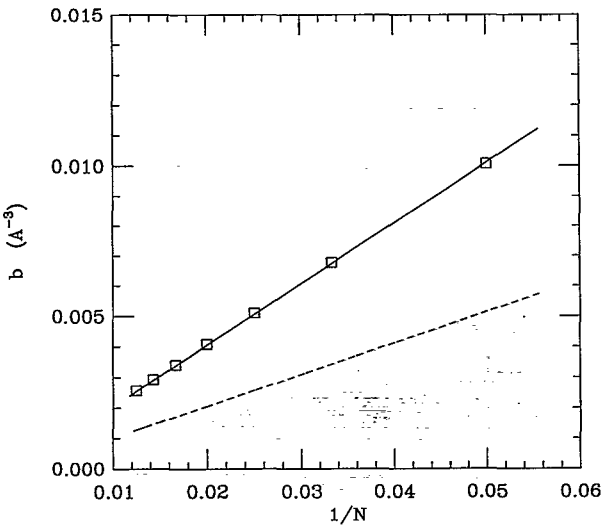

FIG. 14. The same as Fig. 10 for PS/PMMA blends at $P=1.013\times10^5$ Pa and constant N_1/N_2. The solid line corresponds to the least squares fit, while the dashed line illustrates the FH theory prediction.

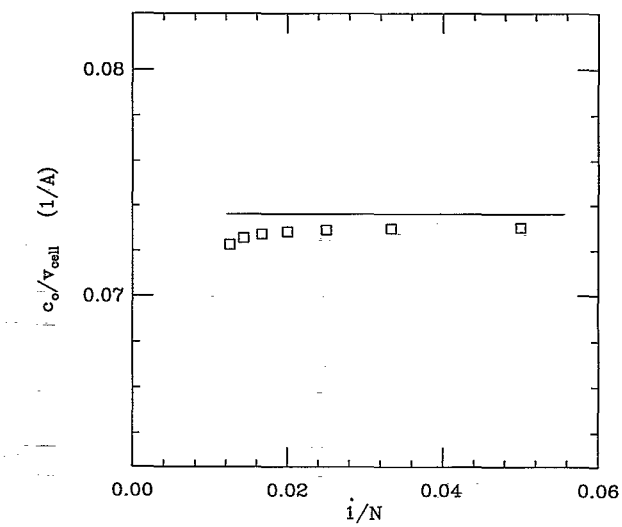

FIG. 15. The same as Fig. 11, but for PS/PMMA blends at $P=1.013\times10^5$ Pa and constant N_1/N_2.

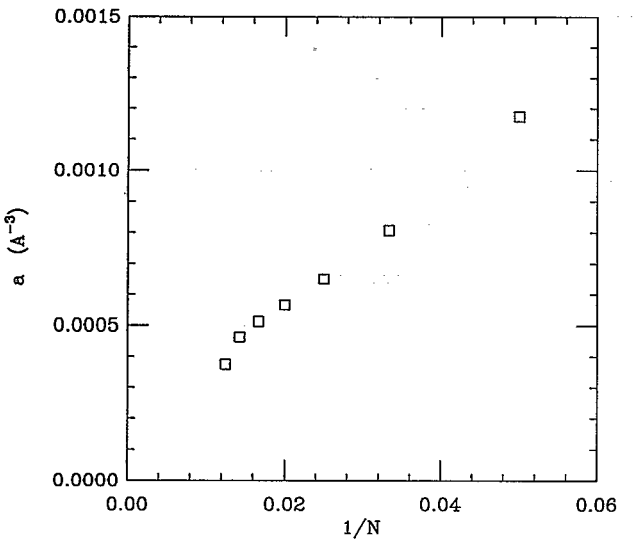

FIG. 16. The same as Fig. 9, but for PS/PMMA blends at $P=1.013\times10^5$ Pa and constant N_1/N_2.

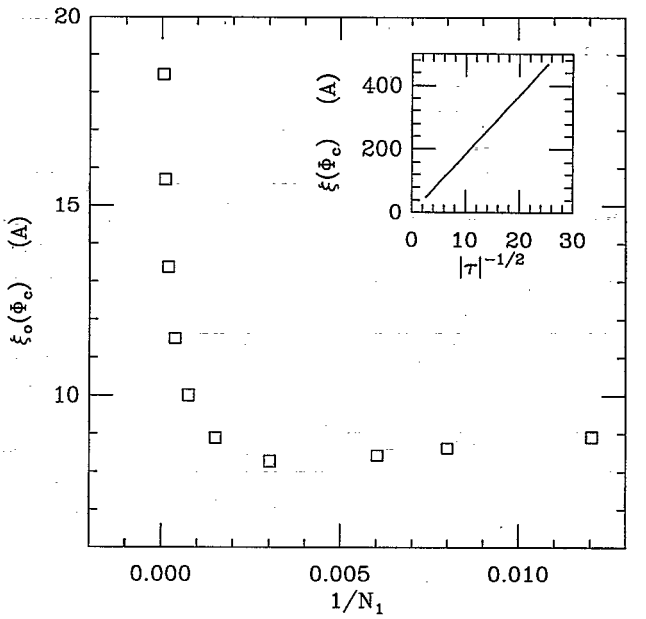

FIG. 17. Lattice cluster theory prediction for the molecular weight dependence of the correlation length amplitude $\xi_0(\Phi_c)$ for PS/PVME blends at $P=1.013\times10^5$ Pa and constant N_1/N_2. The insert shows the linear dependence of the correlation length $\xi(\Phi_c)$ on $|\tau|^{-1/2}$ for a $N_1=21\,180$, $N_2=75\,860$ sample. The reduced temperature τ is defined as $\tau=(T-T_c)/T$.

point. Since for small molecular weight diblock copolymer melts $1/N$ corrections to the free energy from the junction area are very important,[19] the above approximation may lead to a serious error in determining the three microscopic interaction energies $\epsilon_{\alpha\beta}$. Also, the real linking group may have different interaction energies and neglect of this feature may affect the quality of our $\{\epsilon_{\alpha\beta}\}$. Thus, there may be considerable uncertainty to the LCT Ginzburg numbers for PS/PMMA blends. On the other hand, the Ginzburg numbers obtained recently by Maier *et al.*[45] for PS/PMS blends are also very high (0.088–0.36), in accord with LCT computations for PS/PMMA blends. Unfortunately, no experimental data are available for Φ_c, $\chi_{\rm eff}$, ξ, and $S(0)$ of PS/PMMA blends in order to estimate $\mathrm{Gi}^{(\rm inc)}$. Hence, the incompressible RPA equation (3.8), the FH expression (4.1), and Russell's experimental fit[22] $\chi_{\rm eff}=0.028+3.9/T$ are used as an alternative means to determine c_0, Φ_c, and $\chi_{\rm eff}^{\rm ent}$, respectively. The computed $\mathrm{Gi}^{(\rm inc)}$ are the same order of magnitude as the LCT Gi, but the variation of $\mathrm{Gi}^{(\rm inc)}$ with $1/N$ is concave parabolic. Moreover, $\mathrm{Gi}^{(\rm inc)}$ for $N>70$ becomes greater than unity and then suddenly changes in sign. One reason for this unphysical behavior is due to the fact that Russell's data are for a PS-*b*-PMMA diblock copolymer melt, and our LCT demonstrates[19] that $\chi_{\rm eff}$ is N dependent and should differ for blends and blocks. These results again emphasize the necessity of using sufficiently accurate experimental data to generate meaningful Ginzburg numbers from Eq. (4.2). The compressible LCT expressions (3.2), (3.3), (3.6), and (3.15) are clearly superior to Eq. (4.2) for computing Ginzburg numbers. Thus, the compressible LCT provides a much better description of the critical region than the traditional incompressible FH approximation with constant $\chi_{\rm eff}$ and the incompressible RPA.

C. Correlation length amplitude

Equation (3.11) defines the correlation length amplitude $\xi_0(\Phi_c)$ by

$$\xi(\Phi_c,|\tau|\geqslant 0)=\xi_0(\Phi_c)\,|\tau|^{-1/2}.$$

Figure 17 shows the variation of the LCT $\xi_0(\Phi_c)$ with $1/N_1$ for PS/PVME blends. Note that ξ_0 remains nearly constant $\xi_0\sim O(10A)$ for lower molecular weights and then rapidly grows with molecular weights. The insert in Fig. 17 for the representative $N_1=21\,180$ and $N_2=75\,860$ confirms the validity of Eq. (4.3). The LCT computations of ξ_0 are in good accord with the experimental[46] ξ_0 for PS/PVME blends over a range of molecular weights. On the other hand, the molecular weight variation of ξ_0 does not agree with that anticipated from the idealized incompressible RPA theory since ξ_0 would be expected to be generally on the order of the chain radius of gyration. A scaling argument of Sariban and Binder[47] indicates that $\xi_0\sim N^{1-v}$, $v=0.63$ in the critical region. The variation of the LCT ξ_0 with N_1, however, does not even follow a power law unless an artificial force fit is made for the highest molecular weight blends.

It should be emphasized that ξ_0 is a crucial parameter for determining blend properties. Not only does this parameter play a predominant role in governing the width of the nonclassical regime [it appears to the sixth power in Eq. (3.15)], but it is a primary parameter in determining the interfacial tension[48] and the magnitude of hydrodynamic interactions (mode coupling) on the dynamics of phase separation in blends.[49] The assumption that incompressible RPA theory is even qualitatively correct for estimating ξ_0 can lead to gross quantitative errors.

The LCT computations of ξ_0 for PS/PMMA blends in Fig. 18 display a more gradual variation with molecular weight. The temperature dependence of $\xi(\Phi_c)$ is also

found to be quite linear in the reduced temperature τ. Again a simple power law also does not fit molecular weight dependence in Fig. 18.

V. DISCUSSION

Intense current interest is being focused on studies of critical fluctuations in binary polymers blends using small angle neutron scattering experiments. A widely used analysis[8–12] of the experimental data determines the critical region by plotting the inverse zero angle structure factor $S(0,T,\Phi_c)^{-1}$ usually vs the reverse temperature $1/T$ and thereby finding the temperature range $\Delta T \approx T^* - T_c$ for which the plot ceases to be linear. The range ΔT is interpreted as the region where mean field theory breaks down. Most analyses of experimental data involve application of a special limiting case of the Ginzburg criterion that is based on the formula of Bates *et al.*[7]

$$\frac{T^*-T_c}{T}=Cv_m^2\frac{([1/(N_1\Phi_c^3)]+\{1/[N_2(1-\Phi_c)^3]\})^2}{([1/(N_1\Phi_c)]+\{1/[N_2(1-\Phi_c)]\}-2\chi_{\rm eff}^{\rm ent})([R_1^2/(N_1\Phi_c)]+\{R_2^2/[N_2(1-\Phi_c)]\})^3}, \tag{5.1}$$

where R_α is the radius of gyration of a chain of polymer species α, v_m is the average monomer volume, N_α's are polymerization indices, Φ_c is the critical composition of species 1, $\chi_{\rm eff}^{\rm ent}$ is the entropic part of the effective interaction parameter $\chi_{\rm eff}$ as defined by extrapolated zero angle neutron scattering data, and C is a universal constant. However, experiments seem to imply that the constant C in Eq. (5.1) is not universal and varies significantly for different blends.[9] Schwahn *et al.*[9] therefore conclude that the "Ginzburg criterion" of Eq. (5.1) *is not yet fully understood in terms of existing experiments.*

Possible reasons for the nonuniversality of C are manifold. Equation (5.1) is derived assuming the validity of the Flory–Huggins (FH) theory, the constancy of $\chi_{\rm eff}$ with composition and molecular weights, and the validity of the incompressible random phase approximation (RPA). However, it is well known that none of these assumptions underlying the derivation of Eq. (5.1) are indeed met by real polymer blends. The interaction parameter $\chi_{\rm eff}$ is generally found to be composition dependent with possible molecular weight dependences setting in at lower molecular weights. While blend compressibility is low compared to that of gases, blends often have nonzero excess volumes of mixing and they display a rich variety of equations of state. Both of these features are totally ignored by the incompressible FH and RPA theories used to obtain Eq. (5.1). Admitting that polymer blends have composition dependent $\chi_{\rm eff}$ and that "equation of state effects" may influence general thermodynamic derivatives, it is necessary to abandon the simplifying Eq. (5.1) in searches for explanations of the nonuniversality of C and to return to older derivations[5,15,32] of the Ginzburg criterion for the size of the nonclassical regime. These older derivations represent the Ginzburg criterion in terms of the Ginzburg number Gi that is determined by the thermodynamic derivatives a and b and the square gradient term coefficient c_0 which are all to be evaluated at the critical point. There then arises the difficult question of extrapolating experimental data, obtained away from the critical point, to obtain the requisite quantities a and c_0 for evaluation of Gi in Eq. (3.15). If FH and RPA theories were exact, there would be no problem as Eq. (5.1) becomes correct for such an incompressible blend.

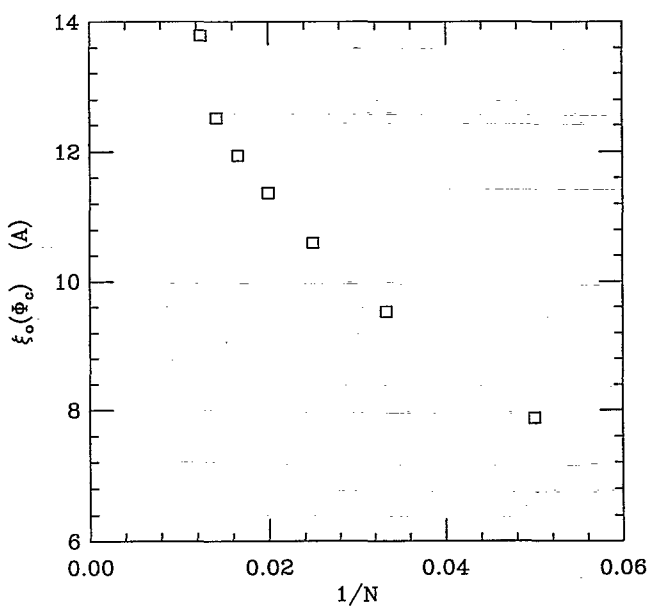

FIG. 18. The same as Fig. 17, but for PS/PMMA blends at $P=1.013\times10^5$ Pa.

Here we use the lattice cluster theory (LCT) to obtain the mean field critical values of a, b, and c_0. The LCT describes compressible blends with structured monomers and includes influences of local correlations and equation of state effects. The LCT is therefore considerably more realistic than the FH and RPA theories of incompressible blends, and consequently, the former theory requires substantially more experimental information and analysis to apply than the zeroth order treatment in Eq. (5.1). Despite the greatly improved representation of reality by the LCT, it is still not perfect as the underlying lattice model clearly suffers from some deficiencies. Nevertheless, we can use the LCT both to compare the predictions of this more realistic approach with the traditional incompressible FH–RPA methods and to establish more realistic trends. In addition,

the LCT computations provide guidance as to the accuracy in using experimental data obtained away from the critical point in the determination of the mean field thermodynamic quantities a and c_0 that govern the width of the nonclassical region.

Figures 9–11 and 14–16 show that compressibility, local correlations, and monomer structure strongly influence a, b, and c_0, often completely altering their molecular weight dependence from those of the FH–RPA theories. Hence, the use of a compressible theory with composition dependent effective interaction parameters is absolutely crucial in formulating an appropriate Ginzburg criterion for polymer blends which are, in fact, compressible and generally have different monomer chemical structures.

The approach of Hair *et al.* [see Eq. (4.2)] uses the same basic theory as leading to Eq. (5.1), but instead represents the right-hand side of this equation in terms of c_0, which is obtained from experimental data using Eq. (3.13), while Φ_c and $\chi_{\rm eff}^{\rm ent}$ are likewise taken from experiments. The use of experimental c_0 and Φ_c represents an improvement over the classic FH–RPA theory of Eq. (5.1), but some differences persist with LCT computations and presumably with reality because the methods of Hair *et al.* do not account for the influence of composition dependent $\chi_{\rm eff}$ and equation of state effects in their implicit extrapolation to the critical regime. Unfortunately, there are only inadequate data to apply in the formula of Hair *et al.* even for the very well-studied case of PS/PVME blends as Gi is quite sensitive to whether the experimental data are obtained for precisely the critical compositions. This forces the use of LCT computations of Φ_c, $\chi_{\rm eff}^{\rm ent}$, and c_0 in order to apply Eq. (4.2). The formula of Hair *et al.* is then found to fare considerably better than the incompressible FH–RPA predictions of Eq. (5.1), but significant quantitative errors remain.

Our LCT calculations indicate that experimental data for $S(0,\Phi_c,T)$, $\xi(\Phi_c,T)$, or $\chi_{\rm eff}(\Phi_c,T)$ may be extrapolated to the critical temperature and produce rather reliable values of the derivative a and the square gradient coefficient c_0. However, these data must be taken for exactly the critical composition, since even a small error in critical parameters can cause a large error in a and c_0. (The knowledge of the critical temperature T_c is also necessary for evaluating τ.) The Gibbs free energy derivative b [see Eq. (3.3)] cannot be extracted from scattering data, and determining it from the incompressible FH theory can lead to significant errors (see Fig. 8).

According to Anisimov *et al.*,[32] other potential reasons exist for the approximate character of the Ginzburg criterion. It may be inappropriate to formulate the Ginzburg criterion in terms of the variable τ as a measure of the distance from the critical point because the critical temperature is shifted by the order parameter fluctuations. Also, the retention in expansion (3.1) of terms through order η^4 only may not be sufficient for analysis in the mean field region away from the critical point. Bearing in mind all these limitations, we have performed computations of the Ginzburg numbers for PS/PVME and PS/PMMA blends as a function of molecular weights. The LCT computations for PS/PVME blends consider ten samples having different polymerization indices $N_{\rm PS}\equiv N_1$ and $N_{\rm PVME}\equiv N_2$, but a constant ratio $N_{\rm PS}/N_{\rm PVME}\equiv N_1/N_2=0.279$. The molecular weight dependence of Gi is, therefore, presented as a function of N_1. A PS/PMMA blend is calculated to be a stable homogeneous phase at normal temperatures for very small molecular weights and, therefore, the polymerization indices for this system are chosen to be equal ($N_1=N_2=N$) and to range between 20 and 80. Our LCT computations indicate a large influence compressibility, local correlations, and monomer structure on Gi and its molecular weight behavior. The Gi scales only as $1/N$ within the simple FH theory, where the effective interaction parameter $\chi_{\rm eff}$ is of purely enthalpic origin. When the effective interaction parameter $\chi_{\rm eff}$ is composed of entropic and enthalpic portions, incompressible FH theory leads to a $1/(N-0.5N^2\chi_{\rm eff}^{\rm ent})$ variation of Gi. The use of a compressible theory, such as the LCT with composition dependent $\chi_{\rm eff}$, produces a Gi which may vary with molecular weights in a very nonmonotonic fashion (see Fig. 8). It, therefore, becomes clear that the resolution of questions concerning the universality of the Ginzburg criterion requires generating further accurate experimental data for near monodisperse blends and also further checking the quality of theories used (in our case the lattice cluster theory).

While the theoretical determination of $\tau_{\rm MF}$ for small molecule liquids is hampered by the complexity of the mean field theory which applies outside the critical region, the case of polymeric fluids is more favorable since mean field scaling is typically exhibited over a wide temperature range outside the critical regime. For example, the recent study of the relatively monodisperse polystyrene–polybutadiene mixture by Hobbie *et al.*[41] finds Gi for this blend as Gi$\approx$0.003, based on Eq. (4.2). Equation (3.18a) then indicates that a deviation from linear behavior should be exhibited about 9.5 °C from the critical temperature. This accords with experimental estimates by Hobbie *et al.*[41] of $\tau_{\rm MF}\approx$9–11 °C (we emphasize again that fluctuation corrections may be significant at this temperature). In spite of the fact that Hobbie *et al.*[41] use incompressible FH theory (with composition independent $\chi_{\rm eff}$) in their estimation of Gi, this agreement is encouraging and similar studies on monodisperse blends would be interesting to check the predictive power of the estimate (3.18a) in determining the breakdown of mean field scaling. These studies must be performed on carefully characterized near monodisperse samples in order to obtain accurate estimates of Gi from the LCT theory. Small errors in the evaluation of the parameters $[\xi_0,S(0),\cdots]$ on which Gi depends can have a large effect on the estimated Ginzburg numbers, so careful experiments are needed for any meaningful discussion of this matter. It should be noted that the temperature control is limited in experiments on real fluids. The best resolution which can be achieved in small molecule liquids corresponds to a reduced temperature $\tau=|T-T_c|/T$ on the order

$$\tau\sim O(10^{-4}-10^{-5}),$$

provided that gravity effects are properly treated. Polymer

blends inevitably have additional limitations on experimental accuracy because of chain polydispersity. If the critical regime is too small to be resolvable by experiment, we then have a mean field fluid for all practical purposes.

ACKNOWLEDGMENTS

This research is supported, in part, by ONR Grant No. N00014-91-J-1442 and DMR Grant No. 92-23804. One of us (J.F.D.) acknowledges useful discussions regarding Eqs. (3.18) with M. Fisher, J. Sengers, and J. M. H. Levelt-Sengers.

[1] P. C. Albright, Z. Y. Chen, and J. V. Sengers, Phys. Rev. B **36**, 877 (1987); G. X. Jin, S. Tang, and J. V. Sengers, Fluid Phase Equilibria **75**, 1 (1992); A. Parola, A. Meroni, and L. Reatto, Int. J. Thermophys. **10**, 345 (1989).
[2] M. R. Moldover and J. S. Gallagher, AIChE. J. **24**, 267 (1978).
[3] P. G. De Gennes, J. Phys. Lett. (Paris) **38**, L441 (1977), J. F. Joanny, J. Phys. A **11**, L117 (1978).
[4] K. Binder, J. Chem. Phys. **79**, 6387 (1983); Phys. Rev. A **29**, 341 (1984).
[5] L. D. Landau and E. M. Lifshitz, *Statistical Physics* (Pergamon, Oxford, 1980), Chap. 14; M. A. Anisimov, *Critical Phenomena in Liquids and Liquid Crystals* (Gordon and Breach, Philadelphia, 1991), Chap. 1.
[6] C. Herkt-Maetzky and J. Schelten, Phys. Rev. Lett. **51**, 896 (1983).
[7] F. S. Bates, J. H. Rosedale, P. Stepanek, T. P. Lodge, P. Wiltzius, G. H. Fredrickson, and R. P. Hjelm, Jr., Phys. Rev. Lett. **65**, 1893 (1990); P. Stepanek, T. P. Lodge, C. Kedrowski, and F. S. Bates, J. Chem. Phys. **94**, 8289 (1991).
[8] S. Janssen, D. Schwahn, and T. Springer, Phys. Rev. Lett. **68**, 3180 (1992).
[9] D. Schwahn, S. Janssen, and T. Springer, J. Chem. Phys. **97**, 8775 (1992).
[10] B. Chu, Q. Ying, K. Linliu, P. Xie, T. Gao, and Y. Li, Macromolecules **25**, 7382 (1992).
[11] D. W. Hair, E. K. Hobbie, A. I. Nakatani, and C. C. Han, J. Chem. Phys. **96**, 9133 (1992).
[12] G. Maier, B. Momper, and E. W. Fischer, J. Chem. Phys. **97**, 5884 (1992).
[13] M. E. Fisher, Phys. Rev. Lett. **57**, 1911 (1986).
[14] J. Dudowicz and K. F. Freed, Macromolecules **24**, 5112 (1991); J. Chem. Phys. **96**, 1644 (1992).
[15] M. Lifschitz, J. Dudowicz, and K. F. Freed (to be published).
[16] I. C. Sanchez and R. H. Lacombe, Macromolecules **11**, 1145 (1978).
[17] H. Tang and K. F. Freed, J. Chem. Phys. **94**, 1572 (1991).
[18] J. F. Douglas (to be published).
[19] K. F. Freed and J. Dudowicz, J. Chem. Phys. **97**, 2105 (1992); J. Dudowicz and K. F. Freed, Macromolecules **26**, 213 (1993).
[20] C. C. Han, B. J. Bauer, J. C. Clark, Y. Muroga, Y. Matsushita, M. Okada, Q. Tran-cong, T. Chang, and I. C. Sanchez, Polymer **29**, 2002 (1988).
[21] T. Shiomi, F. Hamada, T. Nasako, K. Yoneda, K. Imai, and A. Nakajima, Macromolecules **23**, 229 (1990).
[22] T. P. Russell, R. P. Hjelm, Jr., and P. A. Seeger, Macromolecules **23**, 890 (1990).
[23] See, e.g., I. C. Sanchez, J. Appl. Phys. **58**, 2871 (1985).
[24] J. Dudowicz and K. F. Freed (to be published).
[25] J. Dudowicz, K. F. Freed, and W. G. Madden, Macromolecules **23**, 4803 (1990).
[26] J. Dudowicz and K. F. Freed, Macromolecules **24**, 5076 (1991).
[27] J. Dudowicz, M. S. Freed, and K. F. Freed, Macromolecules **24**, 5096 (1991).
[28] K. F. Freed and J. Dudowicz, Theor. Chim. Acta **82**, 357 (1992).
[29] I. C. Sanchez, Macromolecules **24**, 908 (1991).
[30] J. V. Sengers and J. M. H. Levelt-Sengers, in *Progress in Liquid Physics*, edited by C. A. Croxton (Wiley, Chichester, England, 1978), Chap. 4.
[31] A. L. Kholodenko and C. Qian, Phys. Rev. B **40**, 2477 (1989); Phys. Rev. A **42**, 4795 (1990).
[32] M. A. Anisimov, S. B. Kiselev, J. V. Sengers, and S. Tang, Physica A **188**, 487 (1992).
[33] J. Dudowicz and K. F. Freed, J. Chem. Phys. **96**, 9147 (1992).
[34] V. G. Vaks, A. I. Larkin, and S. A. Pikin, Sov. Phys. JETP **24**, 240 (1967).
[35] M. Y. Belyakov and S. B. Kiselev, Physica A **190**, 75 (1992).
[36] Z. G. Wang, A. M. Nemirovsky, K. F. Freed, and K. R. Myers, J. Phys. A **23**, 2575 (1990).
[37] J. F. Douglas and K. F. Freed, Macromolecules **17**, 1854 (1984).
[38] K. F. Freed, *Renormalization Theory of Macromolecules* (Wiley, New York, 1987).
[39] J. M. H. Levelt-Sengers and J. V. Sengers, in *Perspectives in Statistical Physics*, edited by H. J. Raveche (North Holland, Amsterdam, 1981), Chap. 14.
[40] J. V. Sengers (personal communication).
[41] E. K. Hobbie, L. Reed, C. C. Huang, and C. C. Han, Phys. Rev. E (to be published).
[42] H. P. Deutsch and K. Binder (preprint).
[43] A. Yethiraj and K. S. Schweizer, J. Chem. Phys. (to be published).
[44] M. D. Gehlsen, J. H. Rosedale, F. S. Bates, G. D. Wignall, L. Hansen, and K. Almdal, Phys. Rev. Lett. **68**, 2452 (1992)
[45] G. Maier, D. Schwahn, K. Mortensen, and S. Janssen, Europhys. Lett. (to be published).
[46] M. Shibayama, H. Yang, R. S. Stein, and C. C. Han, Macromolecules **18**, 2179 (1985).
[47] A. Sariban and K. Binder, J. Chem. Phys. **86**, 5859 (1987); see also Ref. 42.
[48] H. Chaar, M. R. Moldover, and J. W. Schmidt, J. Chem. Phys. **85**, 418 (1986); M. R. Moldover, Phys. Rev. A **31**, 1022 (1989).
[49] T. Hashimoto, T. Takebe, and S. Suehiro, J. Chem. Phys. **88**, 5874 (1988).